
TUMME: Tsinghua University Minnesota Master Equation program

Rui Ming Zhang,^{a,b} Xuefei Xu,^{*,a} and Donald G. Truhlar^{*,b}

^a*Center for Combustion Energy, Department of Energy and Power Engineering, and Key Laboratory for Thermal Science and Power Engineering of Ministry of Education, Tsinghua University, Beijing 100084, China*

^b*Department of Chemistry, Chemical Theory Center, and Minnesota Supercomputing Institute, University of Minnesota, Minneapolis, Minnesota 55455-0431, USA*

ABSTRACT

TUMME is a program for assembling and solving master equations for gas-phase chemical kinetics based on chemically significant eigenmodes. *TUMME* has interfaces to the *Gaussian*, *Polyrate*, and/or *MSTor* output files that allow the master equation code to provide the microcanonical flux coefficients needed for the coefficient matrix of the master equation. The flux coefficients for reactions with barriers can be calculated by multi-structural variational transition state theory with small-curvature tunneling (MS-VTST/SCT) or by simpler approximations to this such as conventional transition state theory without tunneling (also called RRKM theory). The flux coefficients for barrierless reactions are provided by a hard-sphere model. *TUMME* is written in double precision with Python 3; quadruple and octuple precision are also available for some subtasks in C++. The Python code can run in serial or parallel (MP or MPI), and the C++ code can run on a single processor or on multiple processors with OpenMP.

Program summary

Program Title: TUMME 2.0

CPC Library link to program files: [to be inserted by CPC]

Program also available at: <https://comp.chem.umn.edu/tumme>

Licensing Provisions: Apache-2.0

Programming languages: Python 3 and C++

External libraries: Numpy, Scipy, Numba, mpi4py (optional), modified mpack (optional), qd (optional), omp (optional)

Interfaces to other programs: *Gaussian*, *Polyrate*, and/or *MSTor*

Nature of problem: characterize a temperature-dependent and pressure-dependent complex reaction system

Solution method: solve the energy master equation based on the CSE theory to get phenomenological rate constants and time evolution of the populations.

Features: calculates rate constants and chemically significant eigenmodes; performs calculations by multi-structural variational transition state theory with small-curvature tunneling (MS-VTST/SCT) and/or by simpler theories; can use quadruple or octuple precision; can do calculations in parallel calculations

Keywords

Chemical kinetics

Chemically significant eigenmodes

Master equation
Reaction mechanisms
Torsional anharmonicity
Tunneling
Variational transition state theory

1. INTRODUCTION

The time development of a chemical reaction mechanism involving several species and/or several states can be approximately described as a stochastic process and in particular as a Markov chain.¹ It has long been recognized that this kind of description can be converted to multi-state master equation, and that chemical reaction rate constants can be extracted by eigenanalysis of this master equation.² An especially powerful method, applicable to all unimolecular processes and under many conditions extendable to second-order association reactions, is to linearize the master equation so the eigenvalues have units (s^{-1}) of unimolecular rate constants or pseudo first-order rate constants, and the rate constants can be related to the slowest eigenvalues.^{3,4,5,6,7,8,9,10,11,12,13,14,15,16,17,18,19} An alternative, completely general way to use the master equation for all kinds of reactions is to simulate it by Monte Carlo method for the time-dependent concentrations and extract the rate constants in the same way that one can extract them from experimental data, but for mechanisms involving multiple species, this is less convenient and not always practical to extract the phenomenological rate constants, and it will not be considered further here. Currently, there are several program suites available to solve master equations. The programs *MESS*²⁰ and *MESMER*²¹ are based on eigenanalysis, and *Multiwell*²² is based on the Monte Carlo method.

For the treatment used here, the master equation is discretized in terms of chemical species in finite-width internal energy bins (some works label the bins as grains or intervals). Internal energy in the present context is the total vibrational–rotational energy. For this kind of discretization, the extraction of chemical kinetics rate constants by eigenanalysis has come to be known as the method of chemically significant eigenmodes (CSE theory), and its use for the treatment of complex mechanisms has been greatly developed and clarified in recent years;^{23,24,25,26,27,28,29,30,31,32,33,34} we will build on this work, in particular using the method of Georgievskii et al.³³ This method is applicable to unimolecular isomerization and dissociation reactions proceeding from one or multiple isomers (in the master equation literature, including this paper, “isomers” and “wells” are taken as synonyms). For the case where the concentrations of the bimolecular do not change significantly on the relaxational time scale, association reactions from bimolecular pairs can also be considered.

We note that master equations can also be formulated in a straightforward manner to specify bins in terms of vibrational and rotational quantum numbers (rather than just their total internal energy)^{35,36,37} or in terms of bins specified not only by internal energy E but also by total angular momentum J , leading to the so-called J -conserving master equation,^{38,39,40} but we shall not do this here. It has been estimated that using the simple model used here for energy transfer and bin specification can lead to errors of a factor of two in the predicted rate constants, but one is often willing to accept this accuracy when dealing multi-reaction

mechanisms.⁴¹ When one labels the bins only by internal energy E , one also assumes that reactive flux coefficients depend only on E ; this is a key assumption of the Rice-Ramsperger-Kassel (RRK) theory,^{42,43} of microcanonical transition state theory,^{44,45} and of Rice-Ramsperger-Kassel-Marcus (RRKM) theory,^{46,47,48} which is a special case of microcanonical transition state theory for unimolecular reactions.

A key element of the master equation approach employed here³³ is to identify S unimolecular species γ (also called the wells or isomers), where $\gamma = 1, 2, \dots, S$, and identify m bimolecular pairs ν , where $\nu = 1, 2, \dots, m$. We define $\{\phi\}$ as the union of $\{\gamma\}$ and $\{\nu\}$, where $\phi = 1, 2, \dots, S + m$. We then divide the concentration of isomer γ into N_γ internal energy bins, $\eta = 1, 2, \dots, N_\gamma$, where E_η is the internal energy at the center of bin η . Let $E_{0,\gamma}$ be the zero point energy of isomer γ . Let E_{\max} be the highest internal energy under consideration, and let ΔE be the bin width. Then $E_1 = E_{\max}$, $E_2 = E_{\max} - \Delta E$, $E_3 = E_{\max} - 2\Delta E$, and continuing as long as $E_\eta \geq E_{0,\gamma}$. This gives N_γ energy bins for each isomer.

A key conceptual distinction that is central to CSE theory is the distinction between flux coefficients and rate constants.^{6,9} The treatment used in this paper involves microcanonical flux coefficients as input to build the coefficient matrix of the coupled system of first-order ordinary differential equations, and thermal rate constants corresponding to a given temperature and pressure are computed by eigenanalysis of the coupled system. A microcanonical flux coefficient for a unimolecular reaction is the probability per unit time that an isomer γ in energy bin η , i.e., in state (γ, η) , will make a transition to state (γ', η') or to bimolecular pair ν . A rate constant is the phenomenological constant appearing in a macroscopic rate law involving concentrations summed over all states of a chemical species, where in this paper a chemical species is an isomer or a bimolecular pair.

The program *TUMME* that is described here can be applied to mechanisms that have isomerization reactions (one unimolecular species converting into another), dissociation reactions (a unimolecular species producing a bimolecular pair), and association reactions (a bimolecular pair producing a unimolecular species), but not to mechanisms containing a bimolecular reaction that produces two or more species in a single elementary step. It is not a serious limitation for most applications that *TUMME* does not include elementary reactions (reactions without intermediates) for which both the reactants and the products are bimolecular because one usually makes the assumption that the rate constants of such reactions have negligible nonequilibrium effects and hence do not require simulation by a master equation.

2. Notations and Conventions

Matrices are bold capital letters, e.g., \mathbf{W} , with elements W_{ij} . Diagonal matrices are bold capital letters, e.g., \mathbf{L} , with diagonal elements L_i . Column vectors are bold lower-case letters, e.g., \mathbf{u} with elements u_i . Scalars are italic or Greek. Throughout the presentation, \hat{k} denotes a flux coefficient of an elementary process,^{6,49} and k denotes an observable⁵⁰ rate constant of phenomenological chemical kinetics. Some key notations are summarized in Scheme 1.

γ	index of γ -th isomer
S	number of isomers
η	index of η -th internal energy bin of an isomer

N_γ	number of η for a given γ
i	$(\gamma, \eta) \equiv$ state index, i.e., a specific combination of isomer identity and energy bin
ν	index of ν -th bimolecular pair
$\{\phi\}$	the union of $\{\gamma\}$ and $\{\nu\}$
λ	index of λ -th eigenmode of the symmetrized transition matrix
I	superscript denoting IERE space
C	superscript denoting CSE space
\sim	topmark denoting that a vector or matrix is symmetrized by the \mathbf{F} matrix
\wedge	topmark denoting a flux coefficient to distinguish it from a rate constant
MS	superscript denoting that the value includes multi-structural effects and/or torsional-potential anharmonicity
SSHO	single-structural harmonic oscillator or quasiharmonic oscillator approximation
VTST	variational transition state theory (including CVT and μVT)
CVT	canonical variational theory \equiv canonical VTST
μVT	microcanonical variational theory \equiv microcanonical VTST
GTS	generalized transition state
VTS	variational transition state
\ddagger	conventional transition state
MEP	minimum-energy path
SCT	small-curvature tunneling
ZCT	zero-curvature tunneling
ZPE	zero-point energy (vibrational)
T	superscript denoting a transpose of a matrix
-1	superscript denoting an inverse matrix or elements of an inverse matrix

Scheme 1. Glossary

We use “exergonic” and “endergonic” to refer to the sign of the free energy change in a reaction. We use “exothermic” and “endothermic” to refer to the sign of the enthalpy change in a reaction. “Thermoneutral” means the enthalpy change is zero. We also need language to refer to the potential energy surface. We use “exoergic” and “endoergic” to refer to the sign of the potential energy change. Note the free energies and enthalpies depend on temperature, but the potential energy does not.

We also need a language to discuss energetics of transition states. Free energy of activation and enthalpy of activation refer to the difference of free energy and enthalpy between the transition state and the reactant. The equilibrium structure of a reactant or product is its structure with the lowest potential energy. Conventional transition state theory has a transition state that passes through a saddle, and the saddle point is called the transition structure. The classical barrier height is the difference in potential energy between the saddle point and the equilibrium structure of reactants. Intrinsic barrier is defined as the classical barrier in the exoergic direction. The barrier in the endoergic direction for a reaction with no intrinsic barrier is the positive energy of reaction. Saying that an association reaction is barrierless means that it is exoergic or energetically neutral with no intrinsic barrier. Note that “energy” refers to potential energy in the context of the two previous sentences.

3. THEORY

3.1. Chemically significant eigenmodes

Chemical species always have the possibility of high-energy dissociation reactions (reactions having bimolecular products) with (usually large) positive energies of reaction, and one possibility is that those are not needed in the mechanism. In such a case the resulting mechanism has only isomers, i.e., all forward and reverse reactions are unimolecular, the master equation is first-order and reversible, and the long-time limit of the solution is time-independent equilibrium. If, however, there are dissociation and/or association reactions in the mechanism, one can still set up the master equation to yield the observable isomerization, dissociation, and association rate constants under a reasonably broad set of conditions, and there are two ways to treat the kinetics when bimolecular pairs are present; one is reversible (also called conservative) and leads to equilibrium (and so can be used even if the concentration of isomers at equilibrium is significant), and the other is irreversible (also called nonconservative) and leads to all isomers vanishing because one includes the dissociation reactions but not the reverse association reactions.³³ In this report, when bimolecular pairs are present, we use a version of the irreversible perspective, mainly following the formulation for multiple-well mechanisms by Georgievskii et al.³³ We also assume that a diluent gas is present in excess so that the thermalizing collisions with the bath gas may be treated as collisions with a bath gas of fixed composition, independent of time. When no bimolecular pairs are present the irreversible approach used here reduces to the reversible treatment discussed at the beginning of the paragraph.

The relation between the reversible and irreversible approaches has been discussed in the literature.^{15,24,25,32,33} Both approaches can give the rate constants in terms of eigenvalues associated with chemically significant eigenmodes (CSEs). The reversible approach has the advantage that it can give the concentrations as a function of time for any set of initial concentrations, but the irreversible approach has the advantage that it does not require pseudo-first-order conditions for the products, and it is more convenient for extracting the rate constants in the case of multiwell mechanisms.³³ That is why we use the irreversible approach.

The key variable in the irreversible master equation is the unimolecular concentration vector \mathbf{y} . The concentration of unimolecular species γ in energy bin η is denoted $c_{\gamma\eta}$. We collect the concentrations in each bin of unimolecular species into a vector \mathbf{y} with N_y elements, where the i -th element is

$$y_i \equiv c_{\gamma\eta} \quad (0)$$

All of the bimolecular pairs (if any are to be included in the mechanism) are treated as inhomogeneities that can serve as sources and sinks such that both associations and dissociations can be considered. Then the master equation becomes

$$\frac{d\mathbf{y}}{dt} = -\mathbf{W}\mathbf{y} + \mathbf{b} \quad (1)$$

where t is time, \mathbf{b} is the inhomogeneity, and \mathbf{W} is the transition matrix given by

$$\mathbf{W} = \hat{\mathbf{K}} + \mathbf{P} \quad (2)$$

where $\hat{\mathbf{K}}$ is the unimolecular chemical reaction flux coefficient matrix including isomerization and dissociation (the caret is used to distinguish reactive flux coefficients, which will have carets, from rate constants, which will not), and \mathbf{P} is the collisional energy relaxation matrix. In a later step (see below) one transforms \mathbf{W} to a symmetric matrix \mathbf{G} with positive eigenvalues.

Equation (1) can be rewritten as

$$\frac{dy}{dt} = -\mathbf{W}\mathbf{y} + \mathbf{B}\mathbf{s} \quad (3)$$

where \mathbf{B} is defined such that

$$\left. \frac{dy_i}{dt} \right|_{\text{contribution from association of bimolecular pairs}} = \sum_{v=1}^m B_{iv} s_v \quad (4)$$

and s_v is the product of concentrations of the species A and B

$$s_v = n_A^{(v)} n_B^{(v)} \quad (5)$$

where A and B constitute a bimolecular pair v . Although $n_A^{(v)}$ and $n_B^{(v)}$, and hence s_v , depend on the time, one makes the assumption for the bimolecular pairs that the relaxation time of their internal energy states is fast compared to the time scale of the variation of their concentrations, so \mathbf{B} is treated as independent of time. The matrices $\hat{\mathbf{K}}$, \mathbf{P} , and \mathbf{B} are specified in the next paragraphs.

The matrix $\hat{\mathbf{K}}$ contains the flux coefficients of the isomerization and dissociation reactions:

$$\begin{aligned} \hat{K}_{ii'} &\equiv \hat{K}_{\gamma\eta\gamma'\eta'} \\ &= \begin{cases} \delta_{\gamma\gamma'} \sum_{\phi \neq \gamma} \hat{k}(\gamma \rightarrow \phi | E_\eta) - (1 - \delta_{\gamma\gamma'}) \hat{k}(\gamma' \rightarrow \gamma | E_\eta), & \eta = \eta_i \\ 0, & \end{cases} \quad (6) \end{aligned}$$

where $\hat{k}(\gamma \rightarrow \phi | E_\eta)$ is the microcanonical unimolecular flux coefficient for the reaction $\gamma \rightarrow \phi$ when the internal energy is E_η , and $\hat{k}(\gamma' \rightarrow \gamma | E_\eta)$ is the microcanonical flux coefficient between the γ -th isomer and γ' -th isomer when the internal energy is E_η . These flux coefficients are discussed in Subsection 3.3.

The matrix \mathbf{P} accounts for nonreactive energy transfer collisions with the bath gas:

$$\begin{aligned} P_{ii'} &\equiv P_{\gamma\eta\gamma'\eta'} \\ &= \begin{cases} \omega_\gamma [\delta_{\eta\eta'} - P_\gamma(\eta|\eta')], & \gamma = \gamma' \\ 0, & \gamma \neq \gamma' \end{cases} \quad (7) \end{aligned}$$

where ω_γ is the collision frequency of unimolecular species γ , and $P_\gamma(\eta|\eta')$ is an energy transfer probability for $E_{\eta'} \rightarrow E_\eta$. Further details of this function are in Subsection 3.3.

The matrix \mathbf{B} accounts for association reactions:

$$B_{iv} \equiv B_{\gamma\eta v} = \Delta \hat{k}(v \rightarrow \gamma | E_\eta) \quad (8)$$

where $\Delta \hat{k}(v \rightarrow \gamma | E_\eta)$, which will be precisely defined in Subsection 3.3.2.1, is a generalized microcanonical bimolecular flux coefficient for the bimolecular pair v to form unimolecular species γ with internal energy E_η .

Having formed \mathbf{W} , we symmetrize it based on microscopic reversibility (also called detailed balance); this yields:

$$\mathbf{G} = \mathbf{F}^{-1}\mathbf{W}\mathbf{F} \quad (9)$$

where \mathbf{F} is a diagonal matrix with diagonal elements

$$F_i \equiv F_{\gamma\eta} = \sqrt{\rho_\gamma(E_\eta)\exp(-\beta E_\eta)} \quad (10)$$

where β is $1/(k_B T)$, k_B is Boltzmann's constant, and $\rho_\gamma(E_\eta)$ is the electronic-vibrational-rotational density of states of unimolecular species γ at internal energy E_η . The optical number is also included in $\rho_\gamma(E_\eta)$. We assume the system is in the ground electronic state, but we must include the degeneracy of the electronic ground state in the density of states. Equation (9) produces a symmetric \mathbf{G} .

We label the eigenvalues of \mathbf{G} as L_λ , where λ ranges from 1 to N_y where N_y is the dimension of \mathbf{G} (also the dimension of \mathbf{y}) and equals

$$N_y = \sum_\gamma N_\gamma \quad (11)$$

The eigenvectors of \mathbf{G} are the orthonormal columns $\mathbf{u}^{(\lambda)}$ of a matrix \mathbf{U} that satisfies

$$\mathbf{G}\mathbf{U} = \mathbf{U}\mathbf{L} \quad (12)$$

where

$$L_{\lambda\lambda'} = \delta_{\lambda\lambda'} L_\lambda \quad (13)$$

Thus

$$\mathbf{G}\mathbf{u}^{(\lambda)} = L_\lambda \mathbf{u}^{(\lambda)} \quad (14)$$

Now we transform Eq. (3) to use \mathbf{G} instead of \mathbf{W} . The first step is:

$$\frac{d\mathbf{F}^{-1}\mathbf{y}}{dt} = -\mathbf{F}^{-1}\mathbf{W}\mathbf{y} + \mathbf{F}^{-1}\mathbf{B}\mathbf{s} \quad (15)$$

Substituting Eq. (9) into Eq. (15) yields

$$\frac{d\tilde{\mathbf{y}}}{dt} = -\mathbf{G}\tilde{\mathbf{y}} + \tilde{\mathbf{B}}\mathbf{s} \quad (16)$$

where

$$\tilde{\mathbf{y}} = \mathbf{F}^{-1}\mathbf{y} \quad (17)$$

$$\tilde{\mathbf{B}} = \mathbf{F}^{-1}\mathbf{B} \quad (18)$$

Since the eigenvectors of a real symmetric matrix span the complete space, $\tilde{\mathbf{y}}$ can be expanded as

$$\tilde{\mathbf{y}} = \sum_{\lambda=1}^{N_y} \zeta_\lambda \mathbf{u}^{(\lambda)} \quad (19)$$

where ζ_λ is an expansion coefficient. Substituting Eq. (19) into Eq. (16) and multiplying both sides by the transpose of $\mathbf{u}^{(\lambda)}$, we obtain the following equation:

$$\frac{d\zeta_\lambda}{dt} = -L_\lambda \zeta_\lambda + [\mathbf{u}^{(\lambda)}]^\top \tilde{\mathbf{B}}\mathbf{s} \quad (20)$$

Each term of Eq. (20) is a scalar, and we can write it as

$$\frac{d\zeta_\lambda}{dt} = -L_\lambda \zeta_\lambda + \sum_{i=1}^{N_y} \sum_{v=1}^m u_i^{(\lambda)} F_i^{-1} B_{iv} S_v \quad (21)$$

For simplicity, in the following text, we just use Σ_i as a shorthand for $\sum_{i=1}^{N_y}$.

3.2. Rate Constants

In this subsection we describe how to use the solution to the master equation to provide four kinds of rate constants: isomer-to-isomer, isomer-to-bimolecular pair, bimolecular pair-to-isomer, and bimolecular pair-to-bimolecular pair. The rate constants are all derived under the assumption that internal relaxation is so fast that the state of an isomer is fully described by its internal energy. Furthermore we will find that we can only straightforwardly calculate rate constants when the matrix \mathbf{G} has S small eigenvalues $\lambda = 1, 2, \dots, S$ with eigenvectors corresponding mainly to reactive processes and $N_y - S$ larger eigenvalues with eigenvectors corresponding mainly to internal relaxation. The former set of the eigenvectors constitute the chemically significant eigenmode (CSE) space, and the latter set constitute the internal energy relaxation eigenmode (IERE) space. In *TUMME* we assume the CSE eigenvalues are the S smallest eigenvalues, although this is not necessarily true⁵¹ if the assumed separation of reactive-and-internal-relaxational time scales does not hold. In order to connect the microscopic master equation to the observable macroscopic kinetics, we express the concentration of each isomer as follows:

$$n_\gamma(t) = \sum_{\eta=1}^{N_y} y_{\gamma\eta} = \sum_{\eta=1}^{N_y} F_{\gamma\eta} \tilde{y}_{\gamma\eta} = [\mathbf{h}^{(\gamma)}]^\top \tilde{\mathbf{y}} \quad (22)$$

where $\mathbf{h}^{(\gamma)}$ is the basis vector of unimolecular species γ ; it has the same dimension as $\tilde{\mathbf{y}}$, and its elements are

$$h_{i'}^{(\gamma)} = \delta_{\gamma\gamma'} F_{i'} \quad \text{where } i' = \gamma'\eta' \quad (23)$$

We make the assumption³³ that the vector $\mathbf{h}^{(\gamma)}$ is fully contained in the CSE space, which is orthogonal to the IERE space. With this approximation, substituting Eq. (19) into Eq. (22) yields

$$n_\gamma(t) = \sum_{\lambda=1}^S \zeta_\lambda^C [\mathbf{h}^{(\gamma)}]^\top \mathbf{u}^{(\lambda)} = \sum_{\lambda=1}^S M_{\gamma,\lambda} \zeta_\lambda^C \quad (24)$$

where the superscript C denotes the CSE space. In the rest of the article, the superscript C always denotes the CSE space, and a superscript I denotes the IERE space.

We introduce the $S \times S$ matrix \mathbf{M} with elements

$$M_{\gamma,\lambda} = [\mathbf{h}^{(\gamma)}]^\top \mathbf{u}^{(\lambda)} \quad (25)$$

so that we can write Eq. (24) as

$$\mathbf{n}(t) = \mathbf{M} \boldsymbol{\zeta}^C \quad (26)$$

where $\mathbf{n}(t)$ is an S -dimensional vector containing the concentrations of the isomers; its elements are $n_\gamma(t)$. The matrix \mathbf{M} is a square matrix and is invertible. Thus

$$\boldsymbol{\zeta}^C = \mathbf{M}^{-1} \mathbf{n}(t) \quad (27)$$

and an element of Eq. (27) is

$$\zeta_\lambda^C = \sum_{\gamma'=1}^S (\mathbf{M}^{-1})_{\lambda,\gamma'} n_{\gamma'}(t) \quad (28)$$

where $(\mathbf{M}^{-1})_{\lambda,\gamma'}$ is an element of \mathbf{M}^{-1} , and $\lambda = 1, \dots, S$.

Substituting Eq. (28) and Eq. (5) into Eq. (21) yields

$$\begin{aligned} \sum_{\gamma'=1}^S \frac{(\mathbf{M}^{-1})_{\lambda,\gamma'} dn_{\gamma'}(t)}{dt} \\ = -L_\lambda \sum_{\gamma'=1}^S (\mathbf{M}^{-1})_{\lambda,\gamma'} n_{\gamma'}(t) + \sum_{\nu=1}^m \sum_i u_i^{(\lambda)} F_i^{-1} B_{i\nu} n_A^{(\nu)} n_B^{(\nu)} \end{aligned} \quad (29)$$

Multiplying both sides of Eq. (29) by $M_{\gamma,\lambda}$, and summing over λ from 1 to S , and using

$$\sum_{\lambda=1}^S M_{\gamma,\lambda} (\mathbf{M}^{-1})_{\lambda,\gamma'} = \delta_{\gamma\gamma'} \quad (30)$$

yields

$$\begin{aligned} \frac{dn_\gamma(t)}{dt} = - \sum_{\gamma'=1}^S \left(\sum_{\lambda=1}^S M_{\gamma,\lambda} L_\lambda (\mathbf{M}^{-1})_{\lambda,\gamma'} \right) n_{\gamma'}(t) \\ + \sum_{\nu=1}^m \left(\sum_{\lambda=1}^S M_{\gamma,\lambda} \sum_i u_i^{(\lambda)} F_i^{-1} B_{i\nu} \right) n_A^{(\nu)} n_B^{(\nu)} \end{aligned} \quad (31)$$

We can compare Eq. (31) with the equation defining rate constants in chemical kinetics:

$$\frac{dn_\gamma(t)}{dt} = -k_\gamma n_\gamma(t) + \sum_{\gamma' \neq \gamma} k(\gamma' \rightarrow \gamma) n_{\gamma'}(t) + \sum_{\nu=1}^m k(\nu \rightarrow \gamma) n_A^{(\nu)} n_B^{(\nu)} \quad (32)$$

This comparison identifies the isomerization rate constants $k(\gamma' \rightarrow \gamma)$ and the bimolecular association rate constants $k(\nu \rightarrow \gamma)$ as follows:

$$k(\gamma' \rightarrow \gamma) = -\sum_{\lambda=1}^S M_{\gamma,\lambda} L_\lambda (\mathbf{M}^{-1})_{\lambda,\gamma'} \quad (33)$$

$$k(\nu \rightarrow \gamma) = \sum_{\lambda=1}^S M_{\gamma,\lambda} \sum_i u_i^{(\lambda)} F_i^{-1} B_{i\nu} \quad (34)$$

Next, we derive the dissociation rate constants for forming bimolecular pairs. Under the assumption that the relaxation time scale is much faster than the time scale of variation of the bimolecular concentrations, the solution of Eq. (21) in the IERE space is given by

$$\zeta_\lambda^I = \frac{1}{L_\lambda} \sum_{\nu=1}^m \sum_i u_i^{(\lambda)} F_i^{-1} B_{i\nu} n_A^{(\nu)} n_B^{(\nu)} \quad (35)$$

where $\lambda = S+1, \dots, N_y$. The rate of forming the ν -th bimolecular pair from an arbitrary reactive complex state \mathbf{y} can be expressed as

$$r^{(\nu)} = \sum_i \hat{k}(\gamma \rightarrow \nu | E_\eta) y_i \quad (36)$$

Substituting Eq. (17) and (19) into Eq. (36) yields

$$r^{(\nu)} = \sum_{\lambda=1}^{N_y} \zeta_\lambda \sum_i \hat{k}(\gamma \rightarrow \nu | E_\eta) F_i u_i^{(\lambda)} \quad (37)$$

We can partition the sum in Eq. (37) into CSE and IERE parts:

$$r^{(\nu)} = \sum_{\lambda=1}^S \zeta_\lambda^C \sum_i \hat{k}(\gamma \rightarrow \nu | E_\eta) F_i u_i^{(\lambda)} + \sum_{\lambda=S+1}^{N_y} \zeta_\lambda^I \sum_i \hat{k}(\gamma \rightarrow \nu | E_\eta) F_i u_i^{(\lambda)} \quad (38)$$

Substituting Eq. (28) and Eq. (35) into Eq. (38) yields

$$r^{(\nu)} = \sum_{\gamma'=1}^S \left[\sum_{\lambda=1}^S (\mathbf{M}^{-1})_{\lambda,\gamma'} \sum_i \hat{k}(\gamma \rightarrow \nu | E_\eta) F_i u_i^{(\lambda)} \right] n_{\gamma'}(t) \quad (39)$$

$$+ \sum_{\nu'=1}^m \left[\sum_{\lambda=S+1}^{N_y} \frac{1}{L_\lambda} \left(\sum_{i'} u_{i'}^{(\lambda)} F_{i'}^{-1} B_{i'\nu'} \right) \left(\sum_i \hat{k}(\gamma \rightarrow \nu \mid E_\eta) F_i u_i^{(\lambda)} \right) \right] n_A^{(\nu')} n_B^{(\nu')}$$

We can compare this with the equation defining the phenomenological equations of chemical kinetics,

$$r^{(\nu)} = \sum_{\gamma'=1}^S k(\gamma' \rightarrow \nu) n_{\gamma'}(t) + \sum_{\nu' \neq \nu} k(\nu' \rightarrow \nu) n_A^{(\nu')} n_B^{(\nu')} - k_\nu n_A^{(\nu)} n_B^{(\nu)} \quad (40)$$

This yields the bimolecular pair-to-bimolecular pair rate constant and the unimolecular dissociation rate constant as

$$k(\nu' \rightarrow \nu) = \sum_{\lambda=S+1}^{N_y} \frac{1}{L_\lambda} \left(\sum_{i'} u_{i'}^{(\lambda)} F_{i'}^{-1} B_{i'\nu'} \right) \left(\sum_i \hat{k}(\gamma \rightarrow \nu \mid E_\eta) F_i u_i^{(\lambda)} \right) \quad (41)$$

$$k(\gamma' \rightarrow \nu) = \sum_{\lambda=1}^S (\mathbf{M}^{-1})_{\lambda, \gamma'} \sum_i \hat{k}(\gamma \rightarrow \nu \mid E_\eta) F_i u_i^{(\lambda)} \quad (42)$$

In summary, the four kinds of rate constants are given in Eqs. (33), (34), (41), and (42).

Next we transform the rate constant expressions into matrix form, which is practical for computation. First we rewrite the CSE portion of Eq. (20) in matrix form as

$$\frac{d\boldsymbol{\zeta}^C}{dt} = -\mathbf{L}^C \boldsymbol{\zeta}^C + (\mathbf{U}^C)^\top \tilde{\mathbf{B}} \mathbf{s} \quad (43)$$

where \mathbf{L}^C is a $S \times S$ diagonal matrix whose diagonal elements are the CSE eigenvalues, and \mathbf{U}^C is a $N_y \times S$ matrix whose columns are the CSE eigenvectors. Substituting Eq. (27) into Eq. (43), we can rewrite Eq. (31) as

$$\frac{d\mathbf{n}(t)}{dt} = -\mathbf{M} \mathbf{L}^C \mathbf{M}^{-1} \mathbf{n}(t) + \mathbf{M} (\mathbf{U}^C)^\top \tilde{\mathbf{B}} \mathbf{s} \quad (44)$$

Then we rewrite Eq. (35) as

$$\boldsymbol{\zeta}^I = (\mathbf{L}^I)^{-1} (\mathbf{U}^I)^\top \tilde{\mathbf{B}} \mathbf{s} \quad (45)$$

where \mathbf{L}^I is a $(N_y - S) \times (N_y - S)$ diagonal matrix whose elements are the IERE eigenvalues, and \mathbf{U}^I is an $N_y \times (N_y - S)$ matrix whose columns are the IERE eigenvectors. Using Eqs. (27) and (45), Eq. (38) can be rewritten as

$$\mathbf{r}(t) = \mathbf{D}^\top \mathbf{F} \mathbf{U}^C \mathbf{M}^{-1} \mathbf{n}(t) + \mathbf{D}^\top \mathbf{F} \mathbf{U}^I (\mathbf{L}^I)^{-1} (\mathbf{U}^I)^\top \tilde{\mathbf{B}} \mathbf{s} \quad (46)$$

where \mathbf{D} is the dissociation flux coefficient matrix with elements

$$D_{i\nu} = \hat{k}(\gamma \rightarrow \nu \mid E_\eta).$$

According to Eqs. (44) and (46), the rate constants can be formulated as

$$\begin{aligned} \mathbf{K}_{ww} &= -(\mathbf{M} \mathbf{L}^C \mathbf{M}^{-1})^\top \\ \mathbf{K}_{bw} &= \tilde{\mathbf{B}}^\top \mathbf{U}^C \mathbf{M}^\top \\ \mathbf{K}_{wb} &= (\mathbf{D}^\top \mathbf{F} \mathbf{U}^C \mathbf{M}^{-1})^\top \\ \mathbf{K}_{bb} &= [\mathbf{D}^\top \mathbf{F} \mathbf{U}^I (\mathbf{L}^I)^{-1} (\mathbf{U}^I)^\top \tilde{\mathbf{B}}]^\top \end{aligned} \quad (47)$$

where the subscripts ww, bw, wb, and bb denote unimolecular-to-unimolecular, bimolecular-to-unimolecular, unimolecular-to-bimolecular, and bimolecular-to-bimolecular, respectively, and each \mathbf{K} matrix is a matrix of rate constants, e.g., $(\mathbf{K}_{bw})_{\nu\gamma}$ denotes the rate constant $k(\nu \rightarrow \gamma)$.

In the formulation of master equations (Subsection 3.1) and of rate constants (Subsection 3.2), all bimolecular pairs are treated equally, and they can participate in Eq. (3) as reactants of association reactions (in the matrix \mathbf{B}) and products of dissociation reactions (in diagonal elements of the matrix \mathbf{W}). When no bimolecular pairs are included in the mechanism, Eq. (3) is a set of N_y coupled homogeneous first-order differential equations. When bimolecular pairs are included in the mechanism, it is a set of N_y coupled inhomogeneous first-order differential equations, and the solution depends on the inhomogeneity $\mathbf{B}\mathbf{s}$. The matrix \mathbf{B} is a constant matrix composed of flux coefficients, but the vector \mathbf{s} requires additional considerations. It is important to recall here the assumption made [before Eq. (35)] in deriving the rate constants. Because of this assumption in the derivation, if the bimolecular concentration vector \mathbf{s} is constant on the relaxation time scale, the rate constants depend only on the eigenvalues of \mathbf{G} , and \mathbf{G} – like \mathbf{W} – is independent of \mathbf{s} .

If the time-evolution of \mathbf{y} is needed, we must consider \mathbf{s} . This will be addressed in Subsection 3.5.1.

Since all energy transfer collisions are assumed to occur with the bath gas (i.e., the concentration of bath gas is assumed to be much higher than the concentrations of isomers), the rate constants are independent of the concentrations of isomers, although they do depend on the pressure of the bath gas. The rate constants are also independent of the initial conditions; however the full time evolution of the concentrations in the bins (treated in Subsections 3.5.2 and 5.2) does depend on the initial conditions.

3.3. Transition matrix

The information needed to construct a transition matrix consists of the collision frequency ω_λ , the collisional energy transfer probabilities $P_\gamma(\eta|\eta')$, and the flux coefficients $\hat{k}(\gamma \rightarrow \phi | E_\eta)$ and $\Delta\hat{k}(v \rightarrow \gamma | E_\eta)$. Here we provide the methods used to calculate these quantities.

3.3.1. Collision Model and Energy Transfer Probabilities

The isomer-specific collision frequency ω_γ is estimated as

$$\omega_\gamma = \Omega_{2,2}^* k_{\text{HS}} n_{\text{M}} \quad (48)$$

where $\Omega_{2,2}^*$ is dimensionless reduced collision integral defined by Hirschfelder et al.,⁵² k_{HS} is the hard-sphere collision rate constant, and n_{M} is the concentration of the bath gas. The hard-sphere collision rate constant is

$$k_{\text{HS}} = \pi \left(\frac{d_\gamma + d_{\text{M}}}{2} \right)^2 \sqrt{\frac{8k_{\text{B}}T}{\pi m_{\gamma\text{M}}}} \quad (49)$$

where d_γ and d_{M} are the van der Waals diameters of unimolecular species γ and bath gas M, and $m_{\gamma\text{M}}$ is the reduced mass. The dimensionless reduced collision integral is approximated by fits developed by Troe:⁵³

$$\Omega_{2,2}^* = \begin{cases} \left[0.697 + 0.5185 \log_{10} \left(\frac{k_B T}{\sqrt{\varepsilon_\gamma \varepsilon_M}} \right) \right]^{-1} & \frac{k_B T}{\sqrt{\varepsilon_\gamma \varepsilon_M}} \in [0.3, 3] \\ \left[0.636 + 0.567 \log_{10} \left(\frac{k_B T}{\sqrt{\varepsilon_\gamma \varepsilon_M}} \right) \right]^{-1} & \frac{k_B T}{\sqrt{\varepsilon_\gamma \varepsilon_M}} \in [3, 300] \end{cases} \quad (50)$$

Many models have been developed to calculate the relaxation probability kernel $P_\gamma(\eta|\eta')$; the one used in *TUMME* is the exponential down model⁵⁴ which assumes that the probability of a collision changing the energy of isomer γ from initial energy $E_{\eta'}$ to final energy E_η is:

$$P_\gamma(\eta|\eta') = \begin{cases} A(E_{\eta'}) e^{-\frac{E_{\eta'} - E_\eta}{\langle \Delta E \rangle_d(E_{\eta'})}} & \text{for } E_{\eta'} \geq E_\eta \\ \left[A(E_\eta) e^{-\frac{E_\eta - E_{\eta'}}{\langle \Delta E \rangle_d(E_\eta)}} \right] \frac{\rho_\gamma(E_\eta) e^{-\beta E_\eta}}{\rho_\gamma(E_{\eta'}) e^{-\beta E_{\eta'}}} & \text{for } E_{\eta'} < E_\eta \end{cases} \quad (51)$$

where A is a normalization constant, and $\langle \Delta E \rangle_d(E_{\eta'})$ is the average energy transferred in a collision in which the isomer loses energy to the bath gas, i.e., its energy changes in a downward direction. In most of the literature, $\langle \Delta E \rangle_d$ is taken as a constant or a function of temperature only, but in *TUMME 2.0* we consider both a dependence on the temperature of the bath gas and a dependence on the internal energy of the isomer. In particular we employ the approximation that

$$\langle \Delta E \rangle_d(E_{\eta'}) = \left(\frac{T}{T_c} \right)^n [\alpha(E_{\eta'} - E_{0,\gamma}) + \beta] \quad (52)$$

where T_c , n , α , and β are parameters; and $E_{0,\gamma}$ is the ground-state energy, i.e., the 0 K enthalpy, of isomer γ . We assume parameters T_c , n , α , and β are the same for all isomers. One can of course set α to zero if one does not want to include the internal energy dependence and one can set n to zero if one wants to use a temperature-independent $\langle \Delta E \rangle_d$. Recall that $\eta = 1$ represents the bin with the highest energy E_{\max} , and $\eta' \leq \eta$ implies $E_{\eta'} \geq E_\eta$. The normalization constant is determined by the condition

$$\sum_\eta P_\gamma(\eta|\eta') = 1. \quad (53)$$

The normalization constant is obtained bin-by-bin, starting with $\eta' = 1$, for which all transitions are downward so

$$A(E_1) = \frac{1}{\sum_{\eta=1}^{N_\gamma} e^{-(E_1 - E_\eta)/\langle \Delta E \rangle_d(E_1)}} \quad (54)$$

Then the other $A(E_\eta)$ are obtained recursively by

$$A(E_n) = \frac{1 - \sum_{\eta=1}^{n-1} A(E_\eta) \left[\frac{\rho_\gamma(E_\eta) e^{-\beta E_\eta}}{\rho_\gamma(E_n) e^{-\beta E_n}} \right] e^{-(E_\eta - E_n)/\langle \Delta E \rangle_d(E_n)}}{\sum_{\eta=n}^{N_\gamma} e^{-(E_n - E_\eta)/\langle \Delta E \rangle_d(E_n)}} \quad (55)$$

The procedure is very similar to that employed by Holbrook et al.⁵⁵ Complete details are given in the program manual.

3.3.2. Microcanonical Flux Coefficients

The intrinsic barrier is the potential energy barrier in the exoergic direction of reaction. Reactions without an intrinsic barrier are called barrierless. For reactions with intrinsic barriers, which includes all isomerization reactions and some association/dissociation reactions, anharmonicity, recrossing, and tunneling effects can be included in flux coefficients. The anharmonicity effect is estimated by scaling the vibrational frequencies⁵⁶ and/or by the multi-structural torsional (MS) theory;^{57,58,59,60,61} recrossing effects are included by reaction-path variational transition state theory (VTST),^{62,63,64,65,66} and tunneling is included by small-curvature tunneling (SCT) theory⁶⁷ or Eckart tunneling^{68,69} theory. *TUMME* provides users flexible effects combinations (including neglecting these effects). MS needs a provided *MSTor* output file; VTST and SCT demand a *Polyrate* output file; Eckart tunneling is a program built-in function and needs no external file.

Here we provide a more detailed explanation of the difference between the CVT and μ VT options. We start by reviewing some key terms – generalized transition state (GTS) and variational transition state (VTS). A dividing surface is a hypersurface in phase space (often just in configuration space) that separates reactants from products. The dividing surfaces through points along the minimum-energy path (MEP) are generalized transition states. Only some of these are variational transition states. The actual structures on the MEP are generalized transition structures. Only some of these are variational transition structures. Generalized transition states and generalized transition structures that correspond to local maxima of the generalized free energy of activation for a given temperature are canonical variational transition states and canonical variational transition structures. Generalized transition states and generalized transition structures that correspond to a local minimum of the sum of states up to energy E are respectively microcanonical variational transition states and microcanonical variational transition structures for that energy. We label both canonical variational transition states and microcanonical variational transition states as variational transition states.

The interfaces in *TUMME* to *Polyrate* and *MSTor* only involve their output files, i.e., they are independent of the program packages themselves. If the standard output from *Polyrate* contains the information of generalized transition states along the minimum energy reaction path (geometries, frequencies, energies; the electronic degeneracy and symmetry number will be equal to that of the conventional transition state), the code will read them and calculate the Gibbs free energy or sum of vibrational-rotational states along the reaction path according to canonical variational theory (CVT) or microcanonical variational theory (μ VT) option. Under both options, *TUMME* computes microcanonical flux coefficients as functions of total energy. However, with the CVT option, it places the variational transition state at the location of the canonical variational transition state for the temperature in question, whereas with the μ VT

option it places it at the minimum of the sum over vibrational-rotational states for the given total energy.

For barrierless association and dissociation reactions, flux coefficients are based on a hard-sphere model and only anharmonicity effect is considered here.

These two methodologies are discussed in the next two subsections.

3.3.2.1. Reactions with Barriers

In *TUMME*, in order to include anharmonicity, recrossing, and tunneling into the flux coefficients, we allow for the calculation of the microcanonical flux coefficients by multi-structural variational transition state theory⁷⁰ with small-curvature tunneling (MS-VTST/SCT). Given the output files from *Polyrate* and *MSTor*, *TUMME* can read the minimum energy reaction path, transmission probabilities, and multi-structural torsional densities of states to do the further estimation.

To make the options clear, first need to define two kinds of coefficients, namely microcanonical flux coefficient $\hat{k}^{\text{MS-VTST/SCT}}(\gamma \rightarrow \phi | E_\eta)$ for isomerization or dissociation reactions and the generalized flux coefficient $\Delta\hat{k}^{\text{MS-VTST/SCT}}(\nu \rightarrow \gamma | E_\eta)$ for association reactions.

For isomerization or dissociation reactions, the microcanonical flux coefficient at energy E_η from the γ -th isomer to ϕ -th isomer or bimolecular pair is:⁶⁶

$$\hat{k}^{\text{MS-VTST/SCT}}(\gamma \rightarrow \phi | E_\eta) = \kappa^{\text{SCT}}(E_\eta) \Gamma^{\text{VTST}}(E_\eta) F^{\text{MS}}(E_\eta) \frac{N_{\gamma,\phi}^{\ddagger,\text{SSHO}}(E_\eta)}{h\rho_\gamma^{\text{SSHO}}(E_\eta)} \quad (56)$$

where MS denotes multi-structural; VTST denotes variational transition state theory, which may be canonical variational theory (CVT) or microcanonical variational theory (μ VT); SCT denotes small-curvature tunneling; κ^{SCT} , Γ^{VTST} , and F^{MS} are transmission coefficients; SSHO denotes single-structural harmonic oscillator or single-structural quasiharmonic oscillator; and a dagger (\ddagger) denotes a conventional transition state, i.e., that the transition state properties are evaluated at a dividing surface passing through a saddle point on the potential energy surface.

The transmission coefficients are approximated as follows. The microcanonical MS anharmonicity coefficient is evaluated by

$$F^{\text{MS}}(E_\eta) = \frac{N_{\gamma,\phi}^{\ddagger,\text{MS}}(E_\eta)}{N_{\gamma,\phi}^{\ddagger,\text{SSHO}}(E_\eta)} \frac{\rho_\gamma^{\text{SSHO}}(E_\eta)}{\rho_\gamma^{\text{MS}}(E_\eta)} \quad (57)$$

the microcanonical tunneling coefficient is evaluated by

$$\kappa^{\text{SCT}}(E_\eta) = \frac{N_{\gamma,\phi}^{\ddagger,\text{MS/SCT}}(E_\eta)}{N_{\gamma,\phi}^{\ddagger,\text{MS}}(E_\eta)} \quad (58)$$

and the microcanonical recrossing coefficient is approximated evaluated by

$$\Gamma^{\text{VTST}}(E_\eta) \approx \frac{N_{\gamma,\phi}^{\text{VTS,SSHO/SCT}}(E_\eta)}{N_{\gamma,\phi}^{\ddagger,\text{SSHO/SCT}}(E_\eta)} \quad (59)$$

Note that the numerator of Eq. (59) is evaluated at a variational transition state, and the denominator is evaluated at a conventional transition state. When $N_{\gamma,\phi}(E_\eta)$ is marked with tunneling superscript in Eqs. (58) and (59), it is the cumulative reaction probability (CRP); otherwise it is the sum of states (SoS). When CVT specified, *TUMME* will choose – for each temperature – a variational transition state along the reaction coordinate according to the maximum Gibbs free energy barrier. When μ VT specified, for each energy bin, the program will choose a variational transition state along the reaction coordinate according to the minimum SoS.

The cumulative reaction probability is evaluated as the convolution of the transmission probability with the density of states of the transition state:

$$N_{\gamma,\phi}^{\text{VTS,MS/SCT}}(E_\eta) = \int_{\max\{E_{0,\gamma}, E_{0,\phi}\} - V_a^{\text{G}*}}^{E_\eta - V_a^{\text{G}*}} dE P_{\gamma,\phi}^{\text{SCT}}(E) \rho_{\gamma,\phi}^{\text{VTS,MS}}(E_\eta - E) \quad (60)$$

where E is the energy in the reaction coordinate at VTS which can be negative, $P_{\gamma,\phi}^{\text{SCT}}$ is the small-curvature tunneling (SCT) approximation to the transmission probability of the reaction between γ and ϕ , $\rho_{\gamma,\phi}^{\text{VTS,MS}}$ is the multi-structural torsional electronic-vibrational-rotational density of states of the variational transition state connecting γ and ϕ , and $V_a^{\text{G}*}$, $E_{0,\gamma}$ and $E_{0,\phi}$ are the enthalpy respectively of the variational transition state, of isomer γ , and of isomer or bimolecular pair ϕ at 0 K. The transmission probability $P_{\gamma,\phi}^{\text{SCT}}$ is evaluated by SCT method^{71,72} implemented in *Polyrate*.^{72,73,74} The multi-structural density of states $\rho_{\gamma,\phi}^{\text{VTS,MS}}$ is evaluated as the inverse Laplace transform of the multi-structural torsional partition function with the first-order steepest descent method implemented in *MSTor*.⁵⁷ The derivation of Eq. (60) is given in the Appendix.

The SCT tunneling probability involves the tunneling through an effective potential with an effective reduced mass. The effective potential is the vibrationally adiabatic ground-state potential energy curve given by^{75,76}

$$V_a^{\text{G}} = V_{\text{MEP}}(s) + \epsilon(s) \quad (61)$$

where s is the reaction coordinate (distance along the minimum energy path (MEP) through isoinertial coordinates with reduced mass μ),^{77,78} V_{MEP} is the potential energy along the MEP, and ϵ is the local zero-point energy (ZPE) in vibrational modes transverse to the MEP. The effective mass, μ_{eff} , for SCT is less than μ when the reaction path curvature is nonzero to account for corner-cutting tunneling. Full details of the SCT are given elsewhere.^{71,72}

By analogy to Eq. (60), one can get similar expressions for the CRP with different combinations of effects in Eqs. (56)–(59) by just changing the superscripts. For example, all the SCT superscripts appearing in this text can be replaced by ZCT or Eckart, which respectively denote the zero-curvature tunneling probability^{75,77} calculated by *Polyrate* and the asymmetric Eckart tunneling probability^{68,69} implemented in *TUMME*.

The ZCT approximation differs from SCT in that μ_{eff} is replaced by μ .

The Eckart tunneling approximation used in *TUMME* is the conventional transition state theory approximation to the ZCT approximation. In this method, the vibrationally adiabatic ground-state potential energy curve of the ZCT approximation is replaced by an Eckart barrier as follows.

$$V_a^G = A \frac{\exp\left(\frac{2\pi S}{L}\right)}{1 + \exp\left(\frac{2\pi S}{L}\right)} + B \frac{\exp\left(\frac{2\pi S}{L}\right)}{\left[1 + \exp\left(\frac{2\pi S}{L}\right)\right]^2} \quad (62)$$

where

$$\begin{aligned} A &= \Delta E_{0,f}^\ddagger - \Delta E_{0,r}^\ddagger \\ B &= \left[(\Delta E_{0,f}^\ddagger)^{1/2} + (\Delta E_{0,r}^\ddagger)^{1/2} \right]^2 \\ \frac{L}{2\pi} &= \left(-\frac{2}{F^\ddagger} \right)^{1/2} \left[(\Delta E_{0,f}^\ddagger)^{-1/2} + (\Delta E_{0,r}^\ddagger)^{-1/2} \right]^{-1} \end{aligned} \quad (63)$$

where $\Delta E_{0,f}^\ddagger$ and $\Delta E_{0,r}^\ddagger$ are respectively the 0 K enthalpy of activation (evaluated at the saddle point) of the forward reaction and reverse reaction, and F^\ddagger is the force constant along the reaction coordinate evaluated from the imaginary frequency at the saddle point. Note that this Eckart model involves two important simplifications of the full ZCT model: the effective potential for tunneling is assumed to have its maximum at the saddle point rather than at the maximum of V_a^G , and F^\ddagger is evaluated from V_{MEP} rather than the true V_a^G . Note that eq (62) differs from Ref. 68 because that reference did not include zero-point energies.

For association reactions from bimolecular pair ν to isomer γ , we need to explain the generalized flux coefficient $\Delta \hat{k}^{\text{MS-VTST/SCT}}$ in Eq. (8). From Eq. (4), we obtain

$$\left. \frac{dn_\gamma(t)}{dt} \right|_{\text{contribution from the } \nu\text{-th bimolecular pair}} = s_\nu \sum_{\eta=1}^{N_\gamma} B_{\gamma\eta\nu} \quad (64)$$

Next we assume that all bimolecular pairs are in thermal equilibrium. The microcanonical flux coefficient for association in microcanonical MS-VTST/SCT theory is²⁶

$$\hat{k}^{\text{MS-VTST/SCT}}(\nu \rightarrow \gamma \mid E_\eta) = \Gamma^{\text{VTST}}(E_\eta) \kappa^{\text{SCT}}(E_\eta) F^{\text{MS}}(E_\eta) \frac{N_{\nu,\gamma}^{\ddagger,\text{SSHO}}(E_\eta)}{h\psi_\nu^{\text{SSHO}}(E_\eta)} \quad (65)$$

where $\psi_\nu^{\text{SSHO}}(E_\eta)$ is the density of states per unit energy and per unit volume for the ν -th bimolecular pair, and E_η is the η -th energy bin of product isomer γ . The one-step association rate can be expressed as

$$r(\nu \rightarrow \gamma) = \sum_{\eta=1}^{N_\nu} \hat{k}^{\text{MS-VTST/SCT}}(\nu \rightarrow \gamma \mid E_\eta) \frac{\psi_\nu^{\text{MS}}(E_\eta) e^{-\beta E_\eta} \Delta E}{\Phi_{\text{rel}} Q_\nu^{\text{MS}}} n_A^{(\nu)} n_B^{(\nu)} \quad (66)$$

where Q_ν^{MS} is the electronic-vibrational-rotational partition function of the ν -th bimolecular pair, ΔE is energy step between energy bins, and Φ_{rel} is the relative translational partition function of the bimolecular pair ν . Comparing Eq. (66) with Eq. (64) and substituting Eq. (65) into Eq. (66), we identify the needed function in Eq. (8) as

$$\begin{aligned} B_{\gamma\eta\nu} &\equiv \Delta \hat{k}^{\text{MS-VTST/SCT}}(\nu \rightarrow \gamma \mid E_\eta) \\ &= \Gamma^{\text{VTST}}(E_\eta) \kappa^{\text{SCT}}(E_\eta) F^{\text{MS}}(E_\eta) \frac{N_{\nu,\gamma}^{\ddagger,\text{SSHO}}(E_\eta) e^{-\beta E_\eta} \Delta E}{h\Phi_{\text{rel}} Q_\nu^{\text{SSHO}}} \end{aligned} \quad (67)$$

where $\Gamma^{\text{VTST}}(E_\eta)$ and $\kappa^{\text{SCT}}(E_\eta)$ share the same expression as Eqs. (58), (59) but the $F^{\text{MS}}(E_\eta)$ has a different form as,

$$F^{\text{MS}}(E_\eta) = \frac{N_{\nu,\gamma}^{\ddagger,\text{MS}}(E_\eta)}{N_{\nu,\gamma}^{\ddagger,\text{SSHO}}(E_\eta)} \times \frac{Q_\nu^{\text{SSHO}}(E_\eta)}{Q_\nu^{\text{MS}}(E_\eta)} \quad (68)$$

Here by defining $\hat{k}^{\text{MS-VTST/SCT}}(\gamma \rightarrow \phi \mid E_\eta)$ and $\Delta\hat{k}^{\text{MS-VTST/SCT}}(\nu \rightarrow \gamma \mid E_\eta)$ in Eqs. (56) and (67), we have introduced MS-VTST/SCT theory into master equation. *TUMME* lets user flexibly include any mix combination of MS, VTST and SCT effects. We explicitly expressed Eqs. (56) and (67) as the product of microcanonical recrossing, tunneling and anharmonicity coefficients in order to show user clearly these three effects. Any effect excluded will lead the corresponding coefficient to be 1. If MS is excluded, change the superscript from MS to SSHO; if VTST is excluded, change the superscript from VTS to ‡ (which denotes the conventional transition state passing through the saddle point); if SCT is excluded, change the superscript from SCT into ZCT or Eckart or just delete it. But we note that, unlike the canonical case, in the microcanonical case the recrossing, tunneling and anharmonicity coefficients are coupled rather than independent, e.g., including MS anharmonicity can influence the microcanonical tunneling coefficient.

If no transmission coefficient is employed, the flux coefficient reduces to RRKM theory, which is conventional transition state theory applied to a microcanonical ensemble.^{26,44,45,46,47,48} Then Eq. (56) simplifies to

$$\hat{k}(\gamma \rightarrow \phi \mid E_\eta) = \frac{N_{\gamma,\phi}^\ddagger(E_\eta)}{h\rho_\gamma(E_\eta)} \quad (69)$$

and Eq. (67) simplifies to

$$B_{\gamma\nu} = \Delta\hat{k}(\nu \rightarrow \gamma \mid E_\eta) = \frac{N_{\nu,\gamma}^\ddagger(E_\eta)e^{-\beta E_\eta\Delta E}}{h\Phi_{\text{rel}}Q_\nu} \quad (70)$$

where $N_{\gamma,\phi}^\ddagger(E_\eta)$ and $N_{\nu,\gamma}^\ddagger(E_\eta)$ are the sum of states of the conventional transition state that passes through the lowest-energy saddle point connecting reactants to products. All densities of states, sums of states, and partition functions appearing in Eqs. (69) and (70) are estimated under the harmonic or quasiharmonic single-structure approximation. Note the “quasiharmonic” refers to using the formulas for harmonic oscillators, but with effective frequencies⁵⁶ that may account for anharmonicity or systematic errors in the electronic structure method or both.

3.3.2.2. Barrierless Reactions

Some association reactions are barrierless. A commonly occurring example is the association of a bimolecular pair to a van der Waals complex. The reverse dissociation reaction also has no intrinsic barrier. We use a hard-sphere model to treat barrierless association reactions in the high-pressure limit. Then the microcanonical flux coefficients are calculated by doing an inverse Laplace transform to high-pressure limit canonical flux coefficients.

We label the bimolecular as ν_1 and the complex as γ_1 . The high-pressure limit canonical flux coefficient can be expressed as

$$\begin{aligned} \hat{k}(\gamma_1 \rightarrow \nu_1) &= \frac{1}{Q_{\gamma_1}} \int_0^\infty \hat{k}(\gamma_1 \rightarrow \nu_1 \mid E_\eta) \rho_{\gamma_1}(E_\eta) e^{-\beta E_\eta} dE_\eta \\ &= \frac{\mathcal{L}[\hat{k}(\gamma_1 \rightarrow \nu_1 \mid E_\eta) \rho_{\gamma_1}(E_\eta)]}{Q_{\gamma_1}} \end{aligned} \quad (71)$$

where \mathcal{L} denotes a Laplace transform. The reverse reaction flux coefficient can be obtained through the equilibrium constant.

$$\hat{k}(v_1 \rightarrow \gamma_1) = e^{\beta E_0^{\text{rxn}}} \frac{Q_{\gamma_1}}{\Phi_{\text{rel}} Q_{v_1}} \frac{\mathcal{L}[\hat{k}(v_1 \rightarrow v_1 | E_\eta) \rho_{v_1}(E_\eta)]}{Q_{v_1}} \quad (72)$$

where E_0^{rxn} denotes the reaction energy at 0 K, equaling $E_{0,\gamma_1} - E_{0,v_1}$. Note that for gas-phase species (and *TUMME* only applies to gas-phase reactions), the energy at 0 K is the same as the enthalpy at 0 K. The relative translational partition function is

$$\Phi_{\text{rel}} = \left(\frac{2\pi m_{v_1}}{h^2 \beta} \right)^{\frac{3}{2}} \quad (73)$$

where m_{v_1} is the reduced mass of bimolecular pair v_1 .

One can get the microcanonical flux coefficient by solving Eq. (72) as

$$\hat{k}(v_1 \rightarrow v_1 | E_\eta) = \mathcal{L}^{-1} \left[\hat{k}(v_1 \rightarrow \gamma_1) \Phi_{\text{rel}} e^{-\frac{\Delta E_0^{\text{rxn}}}{RT}} \cdot Q_{v_1} \right] \frac{1}{\rho_{v_1}(E_\eta)} \quad (74)$$

Then, the high-pressure limit flux coefficient $\hat{k}(v_1 \rightarrow \gamma_1)$ is estimated by hard-sphere collision theory as

$$\hat{k}(v_1 \rightarrow \gamma_1) = \pi \left(\frac{d_{v_1}^A + d_{v_1}^B}{2} \right)^2 \sqrt{\frac{8k_B T}{\pi m_{v_1}}} \quad (75)$$

where $d_{v_1}^A$ and $d_{v_1}^B$ are the diameters of two members of bimolecular pair v_1 . Substituting Eq. (75) into Eq. (74), we can derive the flux coefficients that are required as input for barrierless reactions:

$$\hat{k}(v_1 \rightarrow v_1 | E_\eta) = \left[8\pi d_{v_1}^2 \left(\frac{\pi m_{v_1}}{h^2} \right) \int_{E_0^{\text{rxn}}}^{E_\eta} \rho_{v_1}(E_\eta - E) \cdot (E - E_0^{\text{rxn}}) dE \right] \frac{1}{h \rho_{v_1}(E_\eta)} \quad (76)$$

$$\Delta \hat{k}(v_1 \rightarrow \gamma_1 | E_\eta) = \left[8\pi d_{v_1}^2 \left(\frac{\pi m_{v_1}}{h^2} \right) \int_{E_0^{\text{rxn}}}^{E_\eta} \rho_{v_1}(E_\eta - E) \cdot (E - E_0^{\text{rxn}}) dE \right] \frac{e^{-\beta E_\eta} \Delta E}{h \Phi_{\text{rel}} Q_v} \quad (77)$$

Equations (76) and (77) give the flux coefficients for a barrierless reaction between a bimolecular pair and a van der Waals complex. For a barrierless reaction, we do not consider variational effects or tunneling effects, but the multi-structural effect and torsional anharmonicity can be included; thus the density of states and partition function shown in Eqs. (76) and (77) can also be marked with MS superscripts.

3.4. Low-Temperature and High-Temperature Problems

In this section we address two difficulties that are sometimes encountered when we solve the master equation.

The first is that double precision does not always have enough significant figures. This problem arises when the CSE eigenvalues are much smaller than the IERE eigenvalues, which is most likely to happen at low temperature and high pressure and for deep wells. We called this the ‘‘low-temperature problem.’’

The other difficulty is that sometimes one or more of the CSE eigenvalues is not significantly smaller than the smallest IERE eigenvalue. This occurs when the chemical transitions between some species are so fast that the reaction process merges with the relaxation process, i.e., the two time scales become close to one another. This is often occurs at high temperature and for shallow wells or low pressures. We called it “high-temperature problem.”

3.4.1. Low-Temperature Problem

The low-temperature problem can be solved by using a high-precision math library; *TUMME* uses the *qd*⁷⁹ and *mpack*⁸⁰ libraries for this purpose. The original *mpack* library has more capability than is needed for our application because all we need to calculate in high precision are the eigenpairs of a matrix. Thus we simplified *mpack* into a mini version to make the installation process easier.

The precision of a float number is extended to 32 decimal place in quadruple precision and to 64 decimal place in octuple precision. The user should be aware that using high precision can greatly increase the computational cost.

3.4.2. High-Temperature Problem

When the chemical process is not much slower than the relaxation process at high temperatures or very low pressures, the basic assumption used by CSE theory to derive the rate constants becomes invalid.

In Section 3.2, we defined a basis vector $\mathbf{h}^{(\gamma)}$ for each of the S unimolecular species, $\gamma = 1, \dots, S$. The subspace spanned by these basis vectors is called the chemical subspace; the complementary subspace in the space spanned by the eigenvectors of the symmetric transition matrix is the relaxational subspace. In CSE theory, the eigenvectors corresponding to the S lowest eigenvalues should be in the chemical subspaces. However, if equilibration among the chemical species occurs rapidly enough, one or more of the S lowest eigenvalues will become comparable to or greater than the lowest IERE eigenvalue, and their eigenvectors will have a significant component in the relaxational subspace, indicating that two or more species are in relative equilibrium. In such a case, from the point of view of the kinetics, the species in equilibrium with one another should be merged into a single species, and the size of the CSE subspace should be reduced accordingly.

To define a quantity to characterize what fraction of an eigenvector belongs to the CSE space and what fraction belongs to the IERE space, we project the λ -th CSE eigenvector onto the basis vector of the γ -th unimolecular species:

$$EPCS_{\gamma}^{(\lambda)} = \frac{1}{\sqrt{Q_{\gamma}/\Delta E}} [\mathbf{h}^{(\gamma)}]^{\top} \mathbf{u}^{\lambda} = \frac{1}{\sqrt{Q_{\gamma}/\Delta E}} \sum_{i'=1}^{N_y} \delta_{\gamma\gamma'} u_{i'}^{(\lambda)} F_{i'} \quad (78)$$

Equation (77) contains the projection between an eigenvector of the symmetric transition matrix \mathbf{G} and the square root of Boltzmann population; this is equivalent to the projection between the corresponding eigenvector of the asymmetric transition matrix \mathbf{W} and Boltzmann population. The sum of the $EPCS_{\gamma}^{(\lambda)}$ over all isomers (γ) gives the fraction of the λ -th CSE

eigenvector that resides in the CSE space; then the fraction of the λ -th eigenvector belonging to the relaxational subspace is given by

$$P^{(\lambda)} = 1 - \sum_{\gamma} \left[EP C S_{\gamma}^{(\lambda)} \right]^2 \quad (79)$$

where γ is summed over S unimolecular species. The assumptions of CSE theory are well justified only when the $P^{(\lambda)}$ for all CSE eigenvectors are close to zero. Therefore the set of these probabilities serves as an indicator to monitor whether some species need to be merged, i.e., to judge whether the high-temperature problem is occurring.

The high-temperature problem can be remedied by species reduction (SR),⁸¹ which requires finding the species pairs that are in equilibrium and merging them. There is no unique way to assign which species are best treated as equilibrated, but one can try to do this by examining the characters of the eigenmodes. For example, Georgievskii et al.³³ suggest “*For an eigenvector describing equilibration with bimolecular products, the macroscopic population for each unimolecular species has the same sign. For an eigenvector that describes equilibration between two groups of unimolecular species, the cumulative populations for those groups are generally approximately equal in magnitude and opposite in sign, at least at not too high a temperature.*”³³ We next proceed with further considerations of the eigenvectors.

CSE theory assumes that an isomer basis vector $\mathbf{h}^{(\gamma)}$ in the CSE space is orthogonal to the IERE space. However, if an isomer merges with another species, this assumption is not valid, so the right side of Eq. (24) should be augmented with an IERE contribution.

$$n_{\gamma}(t) = \sum_{\lambda=1}^S \zeta_{\lambda}^C [\mathbf{h}^{(\gamma)}]^T \mathbf{u}^{(\lambda)} + \sum_{\lambda=S+1}^{N_y} \zeta_{\lambda}^I [\mathbf{h}^{(\gamma)}]^T \mathbf{u}^{(\lambda)} \quad (80)$$

Substituting Eq. (35) into Eq. (80) yields

$$n_{\gamma}(t) = \sum_{\lambda=1}^S \zeta_{\lambda}^C [\mathbf{h}^{(\gamma)}]^T \mathbf{u}^{(\lambda)} + \sum_{\nu=1}^m \left[\sum_{\lambda=S+1}^{N_y} [\mathbf{h}^{(\gamma)}]^T \mathbf{u}^{(\lambda)} \frac{1}{L_{\lambda}} \sum_i u_i^{(\lambda)} F_i^{-1} B_{i\nu} \right] n_A^{(\nu)} n_B^{(\nu)} \quad (81)$$

When unimolecular species γ is in equilibrium with bimolecular species ν , one has

$$\frac{n_{\gamma}}{n_A^{(\nu)} n_B^{(\nu)}} = \frac{Q_{\gamma}}{\Phi_{\text{rel}} Q_{\nu}} \quad (82)$$

These considerations were used in Ref. 30 to motivate the definition of the following $S \times m$ matrix:

$$\boldsymbol{\kappa} = [\mathbf{H}^T \mathbf{U}^1 (\mathbf{L}^1)^{-1} (\mathbf{U}^1)^T \mathbf{F}^{-1} \mathbf{B}] \circ \mathbf{Q} \quad (83)$$

where \mathbf{H} is a matrix whose columns are the basis vectors \mathbf{h} , where \circ denotes Hadamard product, and the elements of \mathbf{Q} are given by

$$Q_{\gamma,\nu} = \frac{\Phi_{\text{ref}} Q_{\nu}}{Q_{\gamma}} \quad (84)$$

Then an element of $\boldsymbol{\kappa}$ is

$$\kappa_{\gamma,\nu} = \sum_{\lambda=S+1}^{N_y} [\mathbf{h}^{(\gamma)}]^T \mathbf{u}^{(\lambda)} \frac{1}{L_{\lambda}} \sum_i u_i^{(\lambda)} F_i^{-1} B_{i\nu} \frac{\Phi_{\text{ref}} Q_{\nu}}{Q_{\gamma}} \quad (85)$$

and $\kappa_{\gamma,\nu}$ will approach unity when the γ -th isomer and the ν -th bimolecular pair reach equilibrium.

When an isomer merges with another isomer, matrices in the rate constant expression Eq. (47) should be adjusted. First we bind each CSE eigenmode λ' with an isomer γ' in

one-to-one fashion according to Eq. (78). Then, if CSE eigenmode λ' merges into the relaxational subspace, and further the isomer γ' is viewed as being merged into isomer γ'' . The merged eigenmode γ' is moved from the CSE eigenvector matrix \mathbf{U}^C and CSE eigenvalue matrix \mathbf{L}^C into the IERE eigenvector matrix \mathbf{U}^I and IERE eigenvalue matrix \mathbf{L}^I . One row of the matrix \mathbf{M} in Eq. (47) is redefined as

$$M_{\gamma'',\lambda} = \left([\mathbf{h}^{(\gamma')}]^T + [\mathbf{h}^{(\gamma'')}]^T \right) \mathbf{u}^{(\lambda)} \quad (86)$$

where the dimension of matrix \mathbf{M} is reduced from $S \times S$ to $(S - 1) \times (S - 1)$ by deleting the γ' -th row and the λ' -th column and renumbering the remaining CSE eigenvalues with λ ranging from 1 to $S - 1$. The reader is referred to the program manual for more details of the treatment of mergers.

3.5 Time Evolution

3.5.1 Treatments for Bimolecular Species

The master equation in Eq. (3) includes association reactions of bimolecular pairs and dissociation to bimolecular pairs, and – as discussed at the end of Section 3.2 – this requires further consideration when describing the time-varying populations of isomers. There are two possible schemes for calculating the time evolution in the presence of bimolecular pairs:

- (a) *Neglect the inhomogeneities in master equation.* In this scheme, isomers are treated as reactants, and bimolecular pairs in \mathbf{s} are all viewed as product sinks by setting \mathbf{s} constantly equal to 0. Then the time-evolution of \mathbf{y} is obtained by neglecting inhomogeneities in Eq. (3).
- (b) *Add additional equations to describe time-variations of \mathbf{s} .* If some bimolecular pairs are reactants rather than sink-products, i.e., association reactions can occur in these bimolecular pairs, one requires some additional equations for the variation of their concentration. The most common procedure – for each reactant bimolecular pair – is to employ the pseudo-first-order condition that one member of the pair is present in excess, and only the other varies significantly with time. In such a case, there is an additional first-order ODE for each bimolecular pair. The concentration vector \mathbf{y} will contain not only the energy-resolved populations of isomers but also the total concentration of the time-varying member of each reactant bimolecular pair. The transition matrix will also be reorganized to include the association reaction from and the dissociation reactions to the bimolecular reactants.

In *TUMME 2.0*, we only employ the scheme (a) to deal with the time-evolution of concentrations in the bins. Scheme (b) is not included in version 2.0 of *TUMME*.

3.5.2 Time Evolution

The time evolution of the populations of all isomers is derived by solving the set of coupled first-order differential equations in Eq. (16). The inhomogeneity term on the right-hand side of Eq. (16) may contain unknown variables (the concentrations of bimolecular pairs); however, the inhomogeneity term is neglected according to scheme (a) of section 3.5.1, and thus we solve

$$\frac{d\tilde{\mathbf{y}}}{dt} \approx -\mathbf{G}\tilde{\mathbf{y}} \quad (87)$$

Equation (87) has an analytical solution,

$$\tilde{\mathbf{y}}(t) = \mathbf{U}\mathbf{E}\mathbf{U}^T\tilde{\mathbf{y}}_0 \quad (88)$$

where \mathbf{U} is the eigenvector matrix of \mathbf{G} , \mathbf{E} is a diagonal matrix with diagonal elements equal to $e^{-L\lambda t}$, and $\tilde{\mathbf{y}}_0$ is the initial condition. Finally we transform Eq. (88) into concentration units, yielding

$$\mathbf{y}(t) = \mathbf{F}\mathbf{U}\mathbf{E}\mathbf{U}^T\mathbf{F}^{-1}\mathbf{y}_0 \quad (89)$$

4. PROGRAM OVERVIEW

4.1. Work Flow

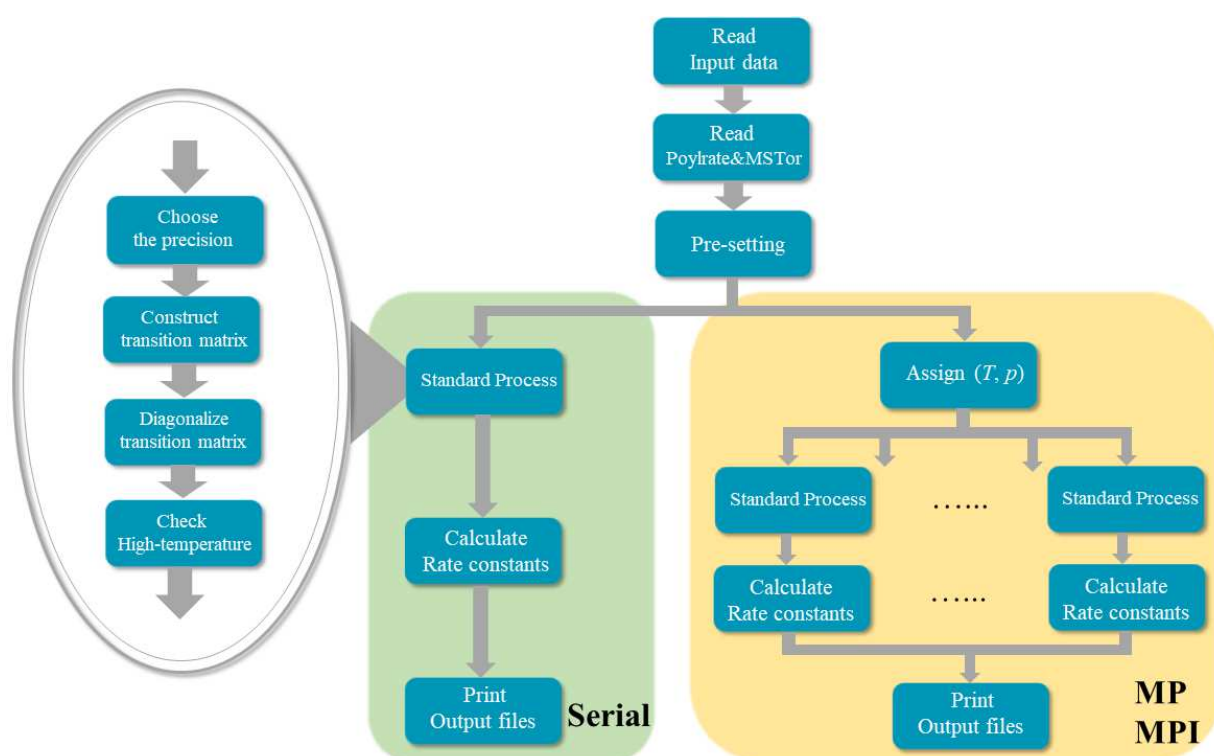


Figure 1. Work flow of TUMME.

The work flow of *TUMME* is depicted as a flowchart in Fig. 1. When the program starts, a standard input file is read to extract global parameters, reaction information, and species properties. If needed, files of *Polyrate* output and of *MSTor* output will be loaded. After some pre-settings like setting the density of states, creating a reaction map, and so forth, the program will enter into the solver part to construct a symmetrized transition matrix and diagonalize it. Before constructing all the matrices in Eq. (47), the program will check whether some species need to be merged. Finally, the rate constants and other information like eigenvectors and eigenvalues will be printed out.

This program is written by Python 3. Python is usually slower than C, C++, or Fortran, but the compatibility of Python across platforms and machines is better. So we sacrificed some speed to make the software easier to use. By employing the scientific computational packages *Numpy*⁸² and *Numba*⁸³, the computational cost in Python is acceptable. In order to further accelerate the program for calculations at multiple temperatures and pressures, we developed a parallel version. The parallel version provides two kinds of parallelism: multi-processing (MP) and message passing interface (MPI). The former can create multiple children threads that can only run within a given node of computer, but the latter can run across a cluster of servers. MP is implemented by the built-in *multiprocessing* module, and MPI is implemented by an external module *mpi4py*⁸⁴. As illustrated in Fig. 1, the parallel scheme is based on the division of the temperatures and pressures. For instance, if the user inputs four temperatures and three pressures and deploys six processors, then each processor handles two conditions of (T, p) .

Sometimes the eigenpairs of the transition matrix can only be calculated accurately by going beyond double precision. Therefore, we modified a simplified version of the high-precision mathematics library *mpack*, and we employed the high-precision float-number library *qd*. With these two libraries, we implemented a quadruple-precision and an octuple-precision version of the standard process in Fig. 1; this implementation uses C++, and we compiled it into a dynamical library. When users choose quadruple and octuple precision option, Python will call the dynamical library. The high-precision library is only developed and debugged for Linux systems.

The parallel and high-precision functionalities are all optional. Users can run the program without them.

4.2. Source Files

The framework of all source files is depicted in Fig. 2. In summary, the main body of the code is written by Python 3, the high precision libraries are implemented by C++. Detailed information about all source files is given in the *TUMME* manual.

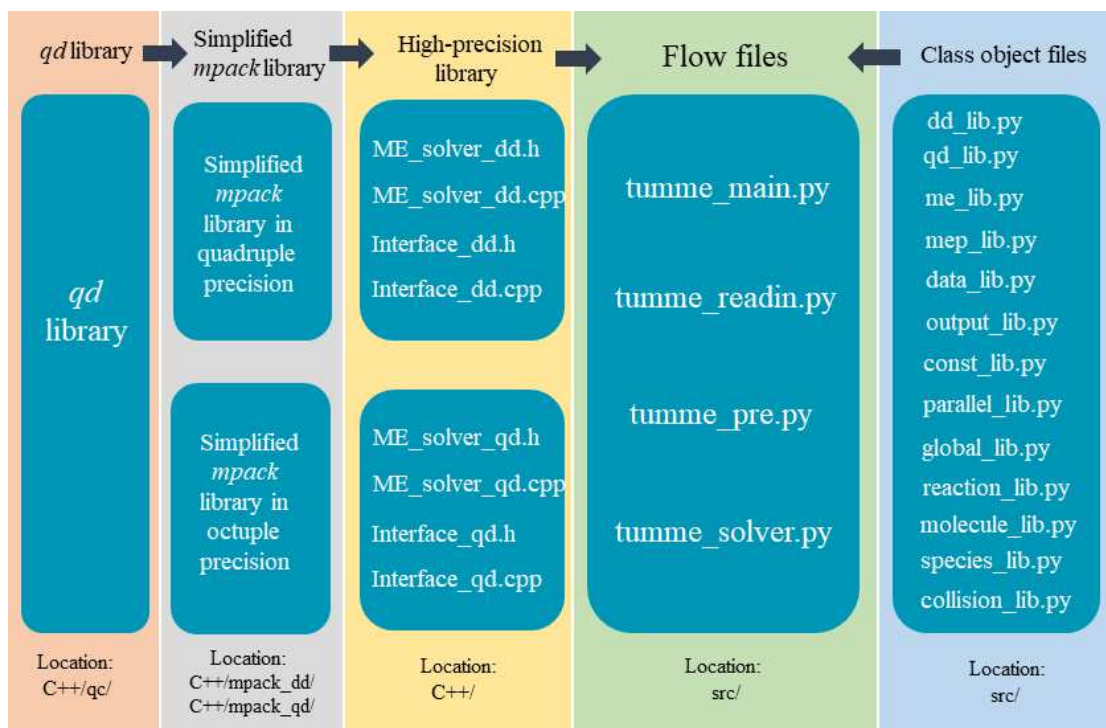


Figure 2. Framework of all source files

5. EXAMPLES OF APPLICATIONS

5.1. Toluene + OH Addition Reactions

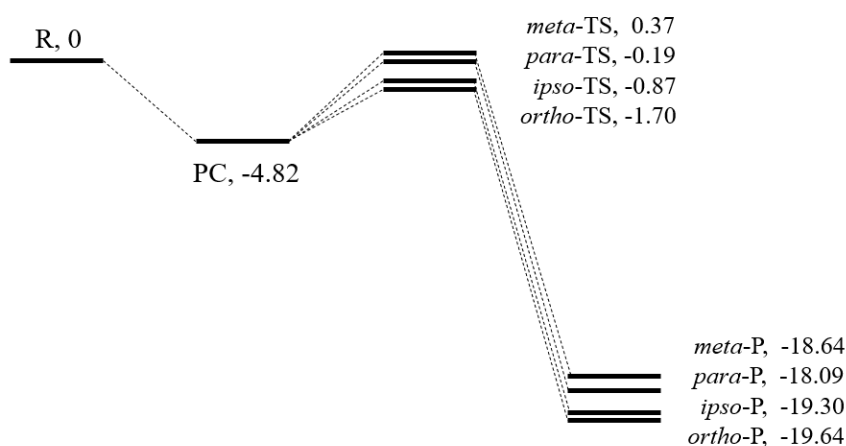


Figure 3. Reaction profile of the toluene + OH addition reactions. The numbers are enthalpies at 0 K relative to the reactant in units of kcal/mol. “R” denotes toluene + OH; “P” denotes C₆H₅OHCH₃; “PC” denotes van der Waals complex.

The first example is the set of four possible addition reactions of OH to toluene.⁸⁵ The pressure for this example is 100 torr with Ar as the bath gas. The geometries, vibrational frequencies, collisions parameters, and energetic quantities are all from the Ref. 85. This example illustrates the recrossing effect, the tunneling effect, and the torsional anharmonicity effect. In our code, we use MS-VTST/SCT theory [$\hat{k}^{\text{MS-CVT/SCT}}(E)$], as described in section 3.3.2.1] to take these effects into consideration. The barrierless reaction from reactant R to the

van der Waals complex PC is estimated as in section 3.3.2.2. The minimum-energy path and transmission probability are calculated by *Polyrate 2016A*⁷³, and the multi-structural torsional density of states is calculated by *MSTor 2017*.⁵⁷ We compare the results to calculations carried out with another program, *MESS*,^{20,33} which is a master equation solver by Georgievskii and Klippenstein. We did a calculation of this reaction in *MESS* to compare the results from different schemes. In the *MESS* calculation, CVT is calculated with the same minimum-energy path from *Polyrate 2016A*, the transmission probability is estimated by the Eckart model with the zero-curvature-tunneling assumption, the torsional anharmonicity is treated using two one-dimensional hindered rotors for internal rotation of HO and CH₃ groups, and the barrierless reaction step of R→PC is estimated by phase space theory. The results from both programs are presented in Fig. 4. The left panel in Fig. 4 shows rate constants of the bimolecular reaction leading to the four addition products. Even though the schemes are different, the results from the two programs are very close. The right panel depicts the sum of the rate constants of the four addition branches. The TST results are from only using conventional RRKM with the SSHO approximation and without tunneling. Although the methods of estimating the flux coefficients in the two codes are different, the results from *MESS* and our code are very similar. We note that in this case the reaction connecting R to PC is so fast that van der Waals complex is merged with the bimolecular pair, and this helps to explain why we obtain approximately the same reaction rates even though we treat the barrierless step differently.

It is encouraging that *TUMME* and *MESS* agree for this example. We expect that there are many cases where multi-structural effects are large^{86,87,88,89} or tunneling effects are very large,⁹⁰ and we anticipate that the high accuracy expected for MS-CVT/SCT in such cases will be very useful.

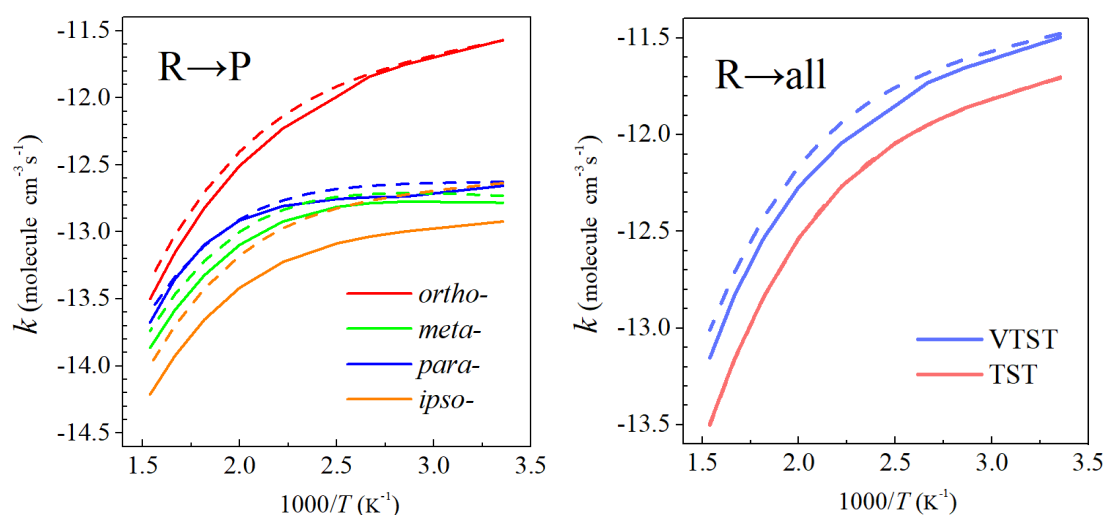


Figure 4. Toluene + OH radical addition reactions at a pressure of 100 torr. The bath gas is Ar. (left panel) Rate constants for the four possible addition reactions of OH to toluene. Solid lines are results by MS-CVT/SCT in *TUMME*, and dashed lines are from a calculation by CVT + Eckart tunneling + hindered rotors carried out in *MESS*. (right panel) TST denotes the sum of the four rate constants by conventional TST (i.e., RRKM) with the SSHO approximation and without tunneling effects (results from both programs are shown, but they are

indistinguishable to plotting accuracy); “VTST” denotes the sum of the four rate constants by each of the two methods in the left panel – with the solid lines from *TUMME* and the dashed line from *MESS*. The barrierless reaction step between R and PC is estimated by phase space theory in *MESS* and by simple collision theory in *TUMME*.

5.2. 2-Methylhexyl Radical Unimolecular Dissociation

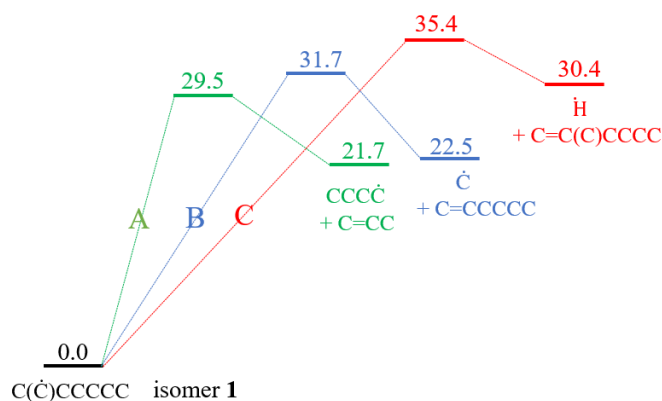


Figure 5. Reaction profiles of three parallel unimolecular dissociation reactions of 2-methylhexyl radical. The numbers are enthalpies at 0 K relative to the reactant in units of kcal/mol. Channel A is colored green, channel B is blue, and channel C is red. The only isomer is called isomer **1**.

The next example reaction, in Fig. 5, illustrates the time evolution of the populations of a reactant isomer (isomer **1**) as obtained in quadruple precision. The reaction system is a parallel set of unimolecular dissociation reactions of the 2-methylhexyl radical,⁹¹ with the products labeled A, B and C. The bath gas is Ar, and all geometries, frequencies, energies and collision parameters are from Ref. 91. The temperature is set at 700 K, and the pressure is 10^{-6} torr.

Because there is only one isomer in this reaction, there is only one CSE eigenvector. So the concentration vector $\mathbf{y}(E_\eta, t)$ is actually the population of energy bins for the isomer **1**. The sum of the elements of $\mathbf{y}(E_\eta, t)$ over energy bins E_η is the concentration of isomer **1**. We set the initial condition to

$$\mathbf{y}_0 = \mathbf{y}(E_\eta, t = 0) = \begin{cases} 1 & \eta = N_\gamma \\ 0 & \text{others} \end{cases} \quad (90)$$

Notice that the units of \mathbf{y}_0 are not specified since they are arbitrary (the results do not depend on absolute values of the isomer concentration under the assumptions stated in Section 3.4.3).

We solved the master equation according to Eq. (89), and the time evolution of the population vector $\mathbf{y}(E_\eta, t)$ is shown in the left panel of Fig. 6. The right panel of Fig. 6 shows the fraction of the concentration that has an energy above the barrier for the given channel; this panel shows clearly how – after a short induction time (< 20 s) – the energetic fractions tend to a steady-state.

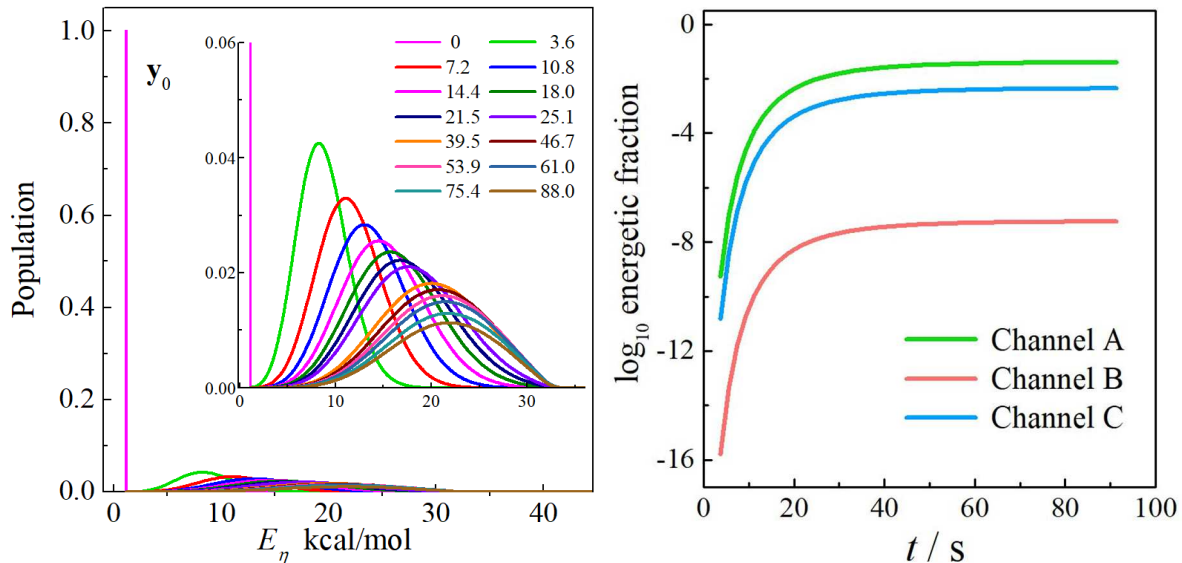


Figure 6. The left panel is the time evolution of population for isomer **1**; y_0 denotes the initial population ($t = 0$), which is 1 for the ground energy bin and 0 for other bins of isomer **1**. The inner figure of the left panel is a zoomed in view of the outer figure. The legend denotes time in a unit of second. The right panel is the time evolution of the “energetic fraction”, which is defined as the fraction ratio of concentration above the channel barrier.

For this single-isomer dissociation reaction, instead of obtaining the steady-state distribution from the time evolution, one can derive it from CSE theory. This gives the CSE-steady-state distribution:

$$g(E_\eta) = \left(\frac{y(E_\eta, t)}{n(t)} \right)_\eta = \frac{\sqrt{\rho(E_\eta) e^{-\beta E_\eta} u(E_\eta)}}{\sum_{E_{\eta'}} \sqrt{\rho(E_{\eta'}) e^{-\beta E_{\eta'}} u(E_{\eta'})}} \quad (91)$$

where $n(t)$ is the concentration of isomer **1**. Even though $y(E_\eta, t)$ and $n(t)$ are time-dependent, the steady-state energy distribution is time-independent. We can also obtain the energetic fraction from the CSE-steady-state distribution Eq. (91) and compare it with what we got from the time evolution of Eq. (89) at times in the steady-state regime; this comparison is shown in Fig.7. We see very good agreement of the two ways of obtaining the steady-state result. Since the CSE-steady-state distribution comes entirely from the one CSE eigenvector, but the steady-state distribution from direct solution involves all the eigenvectors, the good agreement between the solid line and the dashed line in Fig. 7 indicates that the relaxational eigenvectors contribute little to the steady-state distribution. This confirms the basic assumption of CSE theory.

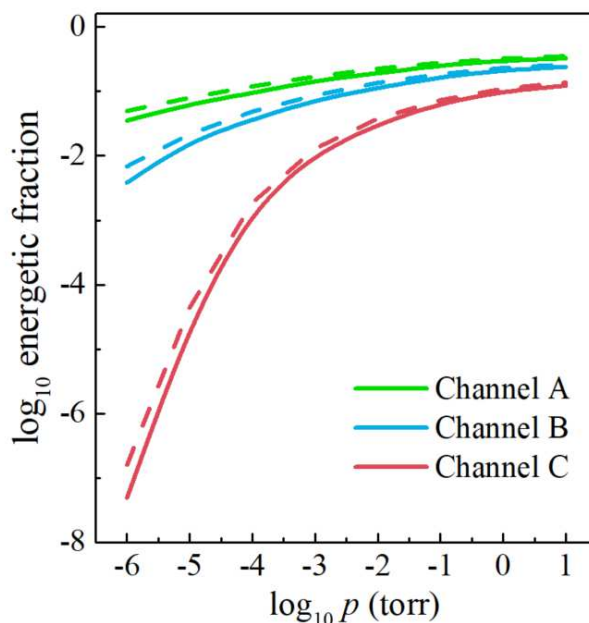


Figure 7. The falloff of the energetic fraction of the steady-state population at 700 K. The solid line results from the direct steady-state solution of Eq. (89). The dashed line is the steady-state population, given by CSE theory, Eq. (91).

The weighted sum of the flux coefficients for producing one of the products in the above case is

$$k_X = \sum_{\eta} k_{X,\text{wt}}(E_{\eta}) \quad (92)$$

where $X = A, B,$ or $C,$ and we have defined

$$k_{X,\text{wt}}(E_{\eta}) = \hat{k}_X(E_{\eta})g(E_{\eta}) \quad (93)$$

Figure 8 illustrates a numerical issue that arises in the present problem because the high-barrier reaction requires high precision. The magnitudes of the components of a normalized eigenvector decrease with increasing energy and eventually, as energy increases, the differences among the magnitudes of the components require a treatment with higher precision. This becomes especially important when there is a high-barrier reaction because the components of the eigenvectors above the barrier may not be accurate. The top panel of Fig. 8 shows that unreliable results are obtained in double precision, and the bottom panel shows that quadruple precision completely overcomes the problem in this case.

This kind of numerical instability differs from what has been discussed in the literature in the past. The well-known case of numerical instability is the low-temperature problem (subsection 3.4.1), where the numerical instability arises from a large difference in magnitudes of the eigenvalues. In the present case though, the numerical instability results from a large difference in the magnitudes of the components of the CSE eigenvectors. Therefore we can add the case of reactions with high barriers to the list of situations where higher precision is needed. This problem can become especially important when one tries to calculate the rate constant for a minor product in a case of competing reactions, where the minor product may have a barrier significantly higher than that of the major product.

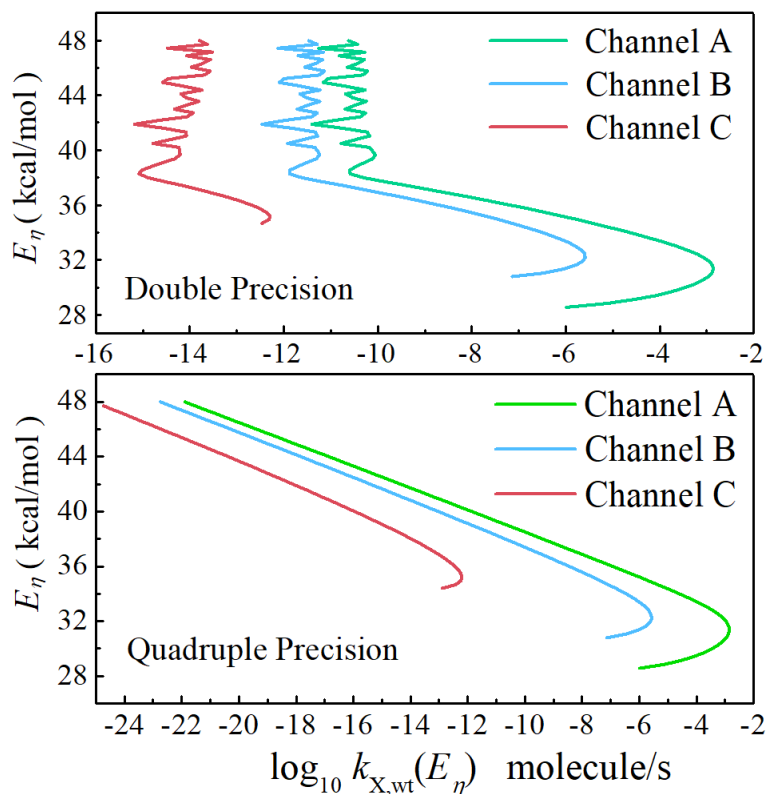


Figure 8. Weighted flux coefficients for dissociation of 2-methylhexyl radicals at 700 K and 10^{-6} torr; see Eq. (93), and note that we set $X = A, B,$ and C . Double precision refers to 8 bytes per word, and quadruple precision refers to 16 bytes per word.

6. CONCLUDING REMARKS

This paper presents a new master equation program for calculating chemical reaction rates based on CSE theory. The formulation involves eigenanalysis of a symmetric transition matrix containing microcanonical flux coefficients. A special feature of the code is that it combines the master equation solution routines with routines to set up the master equation using MS-VTST/SCT theory by reading output files generated by *Gaussian*, *Polyrate*, and/or *MSTor*. One can use quadruple or octuple precision to get accurate eigenpairs even at low temperature or in the case of competing reactions. Two schemes, MP and MPI, are available to parallelize the calculations across multiple temperatures and multiple pressures calculation and decrease the cost.

APPENDIX

Here we consider an elementary reaction $\gamma \rightarrow \phi$ to show how the tunneling is included in the cumulative reaction possibility of Eq. (60), and we show that the result is consistent with CVT/SCT (i.e., with canonical VTST/SCT). The superscript MS will not be indicated in this appendix because the following equations and derivations are valid for both MS and SSHO treatments.

We consider isomer γ to be the reactant. The zero-point energy of the VTS connecting γ and ϕ is ε_0^* . The ground-state energy of the reactant, i.e. of isomer γ , is $E_{0,\gamma}$ (this equals

the sum of the potential energy (the electronic energy) at the minimum-energy geometry of the reactant and the reactant's zero-point energy). We consider a case where $E_{0,\gamma} > E_{0,\phi}$. Let $\varepsilon_{\mathbf{n}}^*$ denote the internal energy at the VTS. We will replace sums over \mathbf{n} at the VTS by integrals over continuous ε^* .

We denote quantities at the VTS by $*$. Then V^* is the potential energy along the MEP at the VTS, and the effective barrier at the VTS is

$$V_{\text{eff}}^* = V^* + \varepsilon^* \quad (\text{A1})$$

The CRP of the VTS without tunneling is

$$N_{\gamma,\phi}^{\text{VTS}}(E_{\eta}) = \sum_{\mathbf{n}} 1 \quad (\text{A2})$$

$$= \int_{\varepsilon_0^*}^{\max(E_{\eta}-V^*, \varepsilon_0^*)} d\varepsilon^* \rho_{\gamma,\phi}^{\text{VTS}}(V_{\text{eff}}^*) \quad (\text{A3})$$

$$= \int_{\varepsilon_0^*}^{\max(E_{\eta}-V^*, \varepsilon_0^*)} d\varepsilon^* \theta(\varepsilon^*) \rho_{\gamma,\phi}^{\text{VTS}}(V_{\text{eff}}^*) \quad (\text{A4})$$

$$= \int_{\varepsilon_0^*}^{\max(E_{\eta}-V^*, \varepsilon_0^*)} d\varepsilon^* \theta(\varepsilon^*) \rho_{\gamma,\phi}^{\text{VTS}}(V^* + \varepsilon^*) \quad (\text{A5})$$

where θ is a Heaviside step function. These equations apply only when $E_{\eta} > E_{0,\gamma}$, although this is not indicated in any of the equations, because $N_{\gamma,\phi}^{\text{VTS}}(E_{\eta})$ is zero by definition when E_{η} is less than $E_{0,\gamma}$ (because there are no reactants with energies that low). Note that

$\rho_{\gamma,\phi}^{\text{VTS}}(V_{\text{eff}}^*)$ is the density of states of the VTS when the total energy is V_{eff}^* , which is another

way to denote the density of states of the VTS when its internal energy is ε^* .

To add tunneling, we replace the step function by a transmission probability (at energies below the effective barrier, this is a tunneling probability). The transmission probability depends on ε^* , which determines the effective potential, and on the total energy E_{η} . Thus

$$N_{\gamma,\phi}^{\text{VTS/SCT}}(E_{\eta}) = \int_{\varepsilon_0^*}^{\infty} d\varepsilon^* P_{\gamma,\phi}^{\text{SCT}}(E_{\eta}; \varepsilon^*) \rho_{\gamma,\phi}^{\text{VTS}}(V^* + \varepsilon^*) \quad (\text{A6})$$

Notice that we also had to change the upper limit of the integral because even though states with $V_{\text{eff}}^* > E_{\eta}$ are not accessible with classical reaction coordinate motion, they are accessible by tunneling when the reaction coordinate is quantum mechanical.

Let's define the energy in the reaction coordinate at the VTS as

$$E = E_{\eta} - V^* - \varepsilon^* = E_{\eta} - V_{\text{eff}}^* \quad (\text{A7})$$

Note that E is negative in the tunneling region and positive when E_{η} is above the effective barrier.

Change the integration variable from ε^* to E gives

$$N_{\gamma,\phi}^{\text{VTS/SCT}}(E_{\eta}) = \int_{-\infty}^{E_{\eta}-V_{\text{a}}^{\text{G}*}} dE P_{\gamma,\phi}^{\text{SCT}}(E_{\eta}; \varepsilon^*) \rho_{\gamma,\phi}^{\text{VTS}}(E_{\eta} - E) \quad (\text{A8})$$

where we used the fact that the minimum value of V_{eff}^* is $V + \varepsilon_0^*$, and we replaced $V^* + \varepsilon_0^*$ by $V_{\text{a}}^{\text{G}*}$, which is simply another name for the same energy.

We now make the assumption that – in the vicinity of the effective-barrier top for a given ε^* – the excited-state vibrationally adiabatic potential curve has the same shape as the ground-state one. Then the tunneling probability depends only on E . We call this the

ground-state tunneling approximation, and we will elaborate on it when we discuss Fig. A2. Then Eq. (A8) becomes

$$N_{\gamma,\phi}^{\text{VTS/SCT}}(E_\eta) = \int_{-\infty}^{E_\eta - V_a^{\text{G}^*}} P_{\gamma,\phi}^{\text{SCT}}(E) \rho_{\gamma,\phi}^{\text{VTS}}(E_\eta - E) dE \quad (\text{A9})$$

Now we can specify the lower limit of Eq. (A9) more precisely. Using the ground-state tunneling approximation, Eq. (A7) becomes

$$E = E_\eta - V_a^{\text{G}^*} \quad (\text{A10})$$

Since E_η has a lower limit of $E_{0,\gamma}$, Eq. (A10) implies that we can change the lower limit in Eq. (A10) as follows:

$$N_{\gamma,\phi}^{\text{VTS/SCT}}(E_\eta) = \int_{-(V_a^{\text{G}^*} - E_{0,\gamma})}^{E_\eta - V_a^{\text{G}^*}} P_{\gamma,\phi}^{\text{SCT}}(E) \rho_{\gamma,\phi}^{\text{VTS}}(E_\eta - E) dE \quad (\text{A11})$$

Eq. (A11) is the same as Eq. (59) because we suppose here that $E_{0,\gamma} > E_{0,\phi}$.

The canonical rate coefficient is

$$k_{\gamma,\phi}^{\text{VTS/SCT}}(T) = \frac{1}{h\Phi Q_\gamma} \int_{E_{0,\gamma}}^{+\infty} N_{\gamma,\phi}^{\text{VTS/SCT}}(E_\eta) e^{-\beta E_\eta} dE_\eta \quad (\text{A12})$$

where Q_γ is the internal partition function of the reactant, i.e. isomer γ ; Φ is the relative translational partition function per unit volume when we are considering a bimolecular reaction and is unity when we are considering a unimolecular reaction; h is Planck's constant; and $\beta \equiv 1/k_B T$. Substituting Eq. (A11) into Eq. (A12) gives

$$k_{\gamma,\phi}^{\text{VTS/SCT}}(T) = \frac{1}{h\Phi Q_\gamma} \int_{E_{0,\gamma}}^{+\infty} dE_\eta \int_{-(V_a^{\text{G}^*} - E_{0,\gamma})}^{E_\eta - V_a^{\text{G}^*}} dE P_{\gamma,\phi}^{\text{SCT}}(E) \rho_{\gamma,\phi}^{\text{VTS}}(E_\eta - E) e^{-\beta E_\eta} \quad (\text{A13})$$

The integration region of this double integral is shown in Fig. A1.

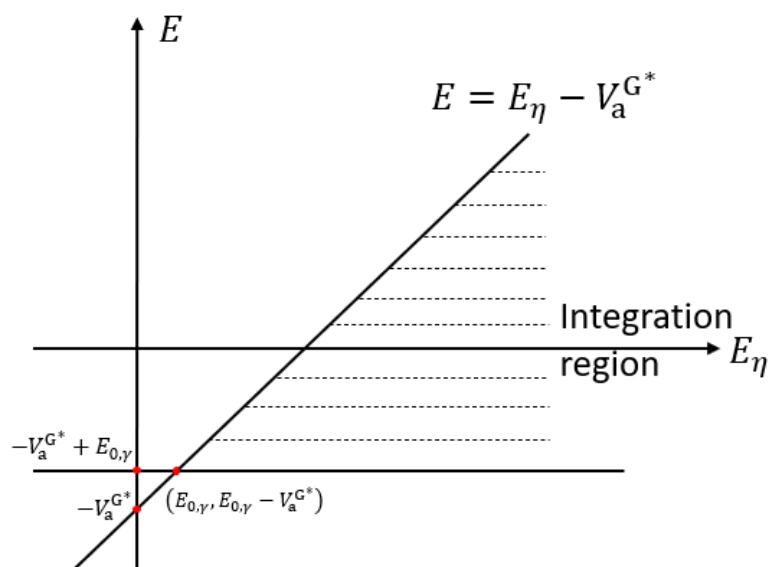


Figure A1. Integration region of the double integral in Eq. (A13).

Based on Fig. A1, we can rewrite the double integral as

$$k_{\gamma,\phi}^{\text{VTS/SCT}}(T) = \frac{1}{h\Phi Q_{\gamma}} \int_{-V_a^{G^*} + E_{0,\gamma}}^{+\infty} P_{\gamma,\phi}^{\text{SCT}}(E) dE \int_{E+V_a^{G^*}}^{+\infty} dE_{\eta} \rho_{\gamma,\phi}^{\text{VTS}}(E_{\eta} - E) e^{-\beta E_{\eta}} \quad (\text{A14})$$

Making a change of variable to

$$E'' = E_{\eta} - E \quad (\text{A15})$$

then gives

$$k_{\gamma,\phi}^{\text{VTS/SCT}}(T) = \frac{1}{h\Phi Q_{\gamma}} \int_{-V_a^{G^*} + E_{0,\gamma}}^{+\infty} P_{\gamma,\phi}^{\text{SCT}}(E) e^{-\beta E} dE \int_{V_a^{G^*}}^{+\infty} dE'' \rho^{\text{VTS}}(E'') e^{-\beta E''} \quad (\text{A16})$$

Recall the definition of the internal partition function:

$$Q_{\gamma,\phi}^{\text{VTS}} = \int_{V_a^{G^*}}^{+\infty} dE'' \rho_{\gamma,\phi}^{\text{VTS}}(E'') e^{-\beta E''} \quad (\text{A17})$$

Thus Eq. (A16) becomes

$$k_{\gamma,\phi}^{\text{VTS/SCT}}(T) = \int_{-V_a^{G^*} + E_{0,\gamma}}^{+\infty} P_{\gamma,\phi}^{\text{SCT}}(E) e^{-\beta E} dE \frac{Q_{\gamma,\phi}^{\text{VTS}}}{h\Phi Q_{\gamma}} \quad (\text{A18})$$

Let

$$E' = E + V_a^{G^*} \quad (\text{A19})$$

to get

$$k_{\gamma,\phi}^{\text{VTS/SCT}}(T) = e^{\beta V_a^{G^*}} \int_{E_{0,\gamma}}^{+\infty} P_{\gamma,\phi}^{\text{SCT}}(E' - V_a^{G^*}) e^{-\beta E'} dE' \frac{Q_{\gamma,\phi}^{\text{VTS}}}{h\Phi Q_{\gamma}} \quad (\text{A20})$$

Our next step is to write Eq. (A20) in terms of the ground-state transmission coefficient P_G^{SCT} that is calculated and printed by *Polyrate*. Figure A2 illustrates the relationship between the tunneling probability in eq. (A20) and the one printed by *Polyrate*.

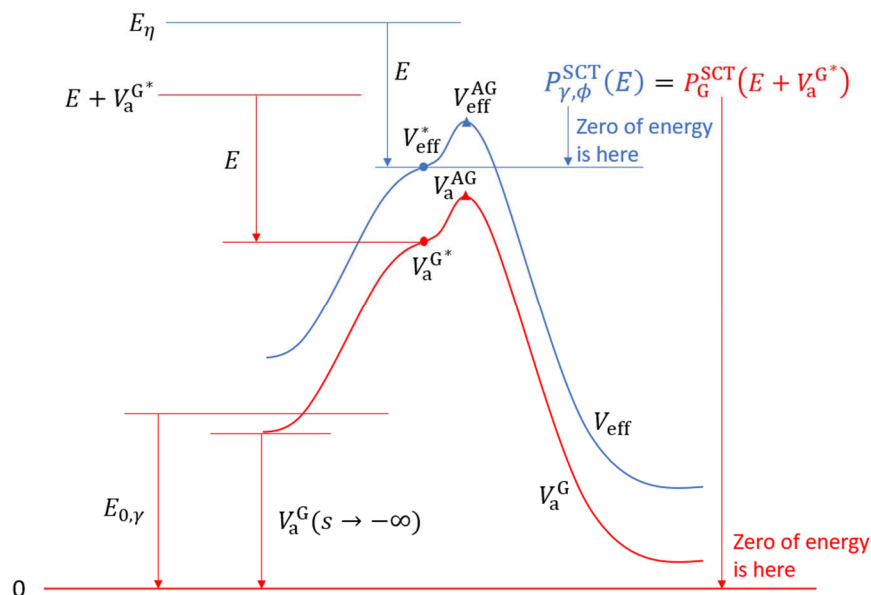


Figure A2. Schematic for the ground-state tunneling approximation. The red curve is the ground-state vibrational adiabatic potential, and the blue curve is a vibrationally-excited-state adiabatic potential. 0 denotes the global ground energy of the whole reaction system. $V_a^G(s \rightarrow -\infty)$ denotes the ground-state vibrational adiabatic potential energy of the reactant.⁹² $P_{\gamma,\phi}^{\text{SCT}}(E)$ is the transmission possibility evaluated by the potential V_{eff} and its argument is the energy relative to the effective potential of the

VTS, V_{eff}^* . $P_{\text{G}}^{\text{SCT}}(E)$ is the transmission possibility evaluated by the potential V_{a}^{G} and its argument is the energy relative to the global ground energy.

As an example showing the meaning of this diagram, suppose $E_{\eta} = 30$, $V_{\text{a}}^{\text{G}^*} = 20$, $V_{\text{a}}^{\text{AG}} = 22$, and $V_{\text{eff}}^* = 25$; then $V_{\text{eff}}^{\text{AG}} = 22 - 20 + 25 = 27$ and $E = 5$. The transmission possibility for the effective potential is $P_{\gamma,\phi}^{\text{SCT}}(E = 5)$, which – with the ground-state tunneling approximation – should equal the transmission probability at an energy 5 units above the ground state of the variational transition state, i.e., $P_{\gamma,\phi}^{\text{SCT}}(E = 5) = P_{\text{G}}^{\text{SCT}}(E + V_{\text{a}}^{\text{G}^*} = 5 + 20 = 25)$. Or in general

$$P_{\gamma,\phi}^{\text{SCT}}(E) = P_{\text{G}}^{\text{SCT}}(E + V_{\text{a}}^{\text{G}^*}) \quad (\text{A21})$$

Substituting Eq. (A21) into Eq. (A20) gives

$$k_{\gamma,\phi}^{\text{VTS/SCT}}(T) = e^{\beta V_{\text{a}}^{\text{G}^*}} \int_{E_{0,\gamma}}^{+\infty} P_{\text{G}}^{\text{SCT}}(E') e^{-\beta E'} dE' \frac{Q_{\gamma,\phi}^{\text{VTS}}}{h\Phi Q_{\gamma}} \quad (\text{A22})$$

which can also be written as

$$k_{\gamma,\phi}^{\text{VTS/SCT}}(T) = \left[\frac{\int_{E_{0,\gamma}}^{+\infty} P_{\text{G}}^{\text{SCT}}(E') e^{-\beta E'} dE'}{\int_{V_{\text{a}}^{\text{G}^*}}^{\infty} e^{-\beta E'} dE'} \right] \frac{1}{\beta h} \frac{Q_{\gamma,\phi}^{\text{VTS}}}{\Phi Q_{\gamma}} \quad (\text{A23})$$

which agrees with the standard expression of canonical rate flux coefficient as given in Eqs. (80) and (85c) of the ‘‘Generalized Transition State Theory’’ book chapter⁹² or Eqs. (49) and (50) in the most recent review paper.⁶⁶

■ AUTHOR INFORMATION

Corresponding Authors

*E-mail: truhlar@umn.edu (DGT), xuxuefei@tsinghua.edu.cn (XX)

ORCID

Rui Ming Zhang: 0000-0002-4880-6391

Donald G. Truhlar: 0000-0002-7742-7294

Xuefei Xu: 0000-0002-2009-0483

■ ACKNOWLEDGMENTS

This work was supported in part by the National Natural Science Foundation of China (awards 21973053 and 91841301) and by the U.S. Department of Energy, Office of Science, Office of Basic Energy Sciences under Award DE-SC0015997.

REFERENCES

- 1 I. Oppenheim and K. E. Shuler, G. H. Weiss, *Physica A* 88A (1977) 191.
- 2 J. Wei and C. D. Prater, *Adv. Catal.* 13 (1962) 203-392.
- 3 B. J. Zwolinski and H. Eyring, *J. Am. Chem. Soc.* 69 (1947) 2702.
- 4 S. K. Kim, *J. Chem. Phys.* 28 (1958) 1057.
- 5 N. S. Snider, *J. Chem. Phys.* 42 (1965) 548.
- 6 B. Widom, *Science* 148 (1965) 1555.
- 7 W. G. Valance and E. W. Schlag, *J. Chem. Phys.* 45 (1966) 216.
- 8 C.A. Brau, *J. Chem. Phys.* 47 (1967) 3076.
- 9 J. T. Bartis and B. Widom, *J. Chem. Phys.* 60 (1974) 3474.
- 10 W. L. Hogarth and D. L. S. McElwain, *J. Chem. Phys.* 63 (1975) 2502.
- 11 A. W. Yau and H. O. Pritchard, *J. Phys. Chem.* 83 (1979) 134.
- 12 C. Lim and D. G. Truhlar, *J. Chem. Phys.* 79 (1983) 3296.
- 13 C. Lim and D. G. Truhlar, *Chem. Phys. Lett.* 114 (1985) 253.
- 14 S. C. Smith, M. J. McEwan and R. G. Gilbert, *J. Chem. Phys.* 90 (1989) 4265.
- 15 M. A. Hanning-Lee, N. J. B. Green, M. J. Pilling and S. H. Robertson, *J. Phys. Chem.* 97 (1993) 860.
- 16 V. M. Bedanov, W. Tsang and M. R. Zachariah, *J. Phys. Chem.* 99 (1995) 11452.
- 17 K. E. Gates, S. H. Robertson, S. C. Smith, M. J. Pilling, M. S. Beasley and K. J. Maschhoff, *J. Phys. Chem. A* 101 (1997) 5765.
- 18 P. K. Venkatesh, A. M. Dean, M. H. Cohen and R. W. Carr, *J. Chem. Phys.* 111 (1999) 8313.
- 19 J. A. Miller, S. J. Klippenstein and S. H. Robertson, *J. Phys. Chem. A* 104 (2000) 7525.
- 20 Y. Georgievskii and S. J. Klippenstein, MESS: Master Equation System Solver (2016). <https://tcg.cse.anl.gov/papr/codes/mess.html>
- 21 S. H. Robertson, D. R. Glowacki, C.-H. Liang, C. Morley, R. Shannon, M. Blitz, P. W. Seakins, M. J. Pilling, MESMER (Master Equation Solver for Multi-Energy Well Reactions), 2008-2013; <http://sourceforge.net/projects/mesmer>.
- 22 J. R. Barker, T. L. Nguyen, J. F. Stanton, C. Aieta, M. Ceotto, F. Gabas, T. J. D. Kumar, C. G. L. Li, L. L. Lohr, A. Maranzana, N. F. Ortiz, J. M. Preses, J. M. Simmie, J. A. Sonk, and P. J. Stimac; MultiWell-v2021 Software Suite; J. R. Barker, University of Michigan, Ann Arbor, Michigan, USA, 2021; <http://clasp-research.engin.umich.edu/multiwell/>.
- 23 S. J. Klippenstein and J. A. Miller, *J. Phys. Chem. A* 106 (2002) 9267.
- 24 J. A. Miller and S. J. Klippenstein, *J. Phys. Chem. A* 107 (2003) 2680.
- 25 J. A. Miller and S. J. Klippenstein, *J. Phys. Chem. A* 108 (2004) 8296.
- 26 A. Fernández-Ramos, J. A. Miller, S. J. Klippenstein and D. G. Truhlar, *Chem. Rev.* 106 (2006) 4518.
- 27 J. A. Miller and S. J. Klippenstein, *J. Phys. Chem. A* 110 (2006) 10528.
- 28 S. H. Robertson, M. J. Pilling, L. C. Jitariu and I. H. Hillier, *Phys. Chem. Chem. Phys.* 9 (2007) 4085.
- 29 J. A. Miller, S. J. Klippenstein, S. H. Robertson, M. J. Pilling and N. J. B. Green, *Phys.*

- Chem. Chem. Phys. 11 (2009) 1128.
- 30 J. W. Allen, C. F. Goldsmith and W. H. Green, Phys. Chem. Chem. Phys. 14 (2012) 1131.
- 31 M. J. Pilling, J. Phys. Chem. A 117 (2013) 3697.
- 32 J. A. Miller and S. J. Klippenstein, Phys. Chem. Chem. Phys. 15 (2013) 4744.
- 33 Y. Georgievskii, J. A. Miller, M. P. Burke and S. J. Klippenstein, J. Phys. Chem. A 117 (2013) 12146.
- 34 J. A. Miller, S. J. Klippenstein, S. H. Robertson, M. J. Pilling, R. Shannon, J. Zádor, A. W. Jasper, C. F. Goldsmith and M. J. Burke, J. Phys. Chem. A 120 (2016) 306.
- 35 J. E. Dove, D. G. Jones and H. Teitelbaum, Proc. Symp. (Int.) Combustion 14 (1973) 177.
- 36 K. Haug, D. G. Truhlar and N. C. Blais, J. Chem. Phys. 86 (1987) 2697.
- 37 S. P. Sharma and D. W. Schwenke, J. Thermophys. Heat Transfer 5 (1991) 469.
- 38 R. G. Gilbert and S. C. Smith, Theory of Unimolecular and Recombination Reactions (Blackwell Scientific Publications, Oxford, 1990), chapter 6.
- 39 A. W. Jasper, K. M. Pelzer, J. A. Miller, E. Kamarchik, L. B. Harding and S. J. Klippenstein, Science 346 (2014) 1212.
- 40 T. L. Nguyen and J. F. Stanton, J. Phys. Chem. A 124 (2020) 2907.
- 41 A. W. Jasper, Int. J. Chem. Kinet. 52 (2020) 387.
- 42 O. K. Rice and H. C. Ramsperger, J. Am. Chem. Soc. 49 (1927) 1618.
- 43 L. S. Kassel, Proc. Nat. Acad. Sci. USA 14 (1928) 23.
- 44 J. L. Magee, Proc. Nat. Acad. Sci. USA 38 (1952) 764.
- 45 J. C. Giddings and H. Eyring, J. Chem. Phys. 22 (1954) 538.
- 46 R. A. Marcus, J. Chem. Phys. 20 (1952) 359.
- 47 H. M. Rosenstock, M. B. Wallenstein, A. L. Wahrhaftig and H. Eyring, Proc. Natl. Acad. Sci. USA 36 (1952) 667.
- 48 R. A. Marcus, J. Chem. Phys. 45 (1966) 2630.
- 49 C. Lim and D. G. Truhlar, J. Phys. Chem. 87 (1983) 2683.
- 50 K. J. Laidler, Chemical Kinetics, 3rd ed. (McGraw-Hill, New York 1987), chapter 1.
- 51 C. Lim and D. G. Truhlar, J. Phys. Chem. 89 (1985) 5.
- 52 J. O. Hirschfelder, C. F. Curtiss and R. B. Bird, Molecular Theory of Gases and Liquids (Wiley, London, 1967).
- 53 J. Troe, J. Chem. Phys. 66 (1977) 4758.
- 54 M. J. Pilling and S. H. Robertson, Annu. Rev. Phys. Chem. 54 (2003) 245
- 55 K. A. Holbrook, M. J. Pilling and S. H. Robertson, Unimolecular reactions, 2nd ed. (Wiley, Chichester, 1996) pp. 198-200.
- 56 I. M. Alecu, J. Zheng, Y. Zhao and D. G. Truhlar, J. Chem. Theory Comput. 6 (2010) 2872.
- 57 J. Zheng, T. Yu, E. Papajak, I. M. Alecu, S. L. Mielke and D. G. Truhlar, Phys. Chem. Chem. Phys. 13 (2011) 10885.
- 58 J. Zheng and D. G. Truhlar, J. Chem. Theory Comput. 9 (2013) 1356.
- 59 J. Zheng, S. L. Mielke, J. L. Bao, R. Meana-Pañeda, K. L. Clarkson and D. G. Truhlar, MSTor computer program, version 2017-A, University of Minnesota, Minneapolis, MN (2017).

-
- 60 J. Zheng, S. L Mielke, K. L Clarkson and D. G. Truhlar, *Computer Phys. Commun.* 183 (2012) 1803.
- 61 J. Zheng, R. Meana-Pañeda and D. G. Truhlar, *Computer Phys. Commun.* 184 (2013) 2032.
- 62 B. C. Garrett and D. G. Truhlar, *Acc. Chem. Res.* 13 (1980) 440.
- 63 B. C. Garrett and D. G. Truhlar, *J. Phys. Chem.* 83 (1979) 1079.
- 64 A. D. Isaacson, M. T. Sund, S. N. Rai and D. G. Truhlar, *J. Chem. Phys.* 82 (1985) 1338.
- 65 A. Fernandez-Ramos, B. A. Ellingson, B. C. Garrett and D. G. Truhlar, *Rev. Comp. Chem.* 23 (2007) 125.
- 66 J. L. Bao and D. G. Truhlar, *Chem. Soc. Rev.* 46 (2017) 7548
- 67 R. T. Skodje, D. G. Truhlar and B. C. Garrett, *J. Phys. Chem.* 85 (1981) 3019
- 68 H. S. Johnston and J. Heicklen, *J. Phys. Chem.* 66 (1962) 532.
- 69 B. C. Garrett and D. G. Truhlar, *J. Phys. Chem.* 83 (1979) 2921.
- 70 T. Yu, J. Zheng and D. G. Truhlar, *Chem. Sci.* 2 (2011) 2199.
- 71 Y.-P. Liu, G. C. Lynch, T. N. Truong, D.-h. Lu, D. G. Truhlar and B. C. Garrett, *J. Am. Chem. Soc.* 115 (1993) 2408.
- 72 D.-h. Lu, T. N. Truong, V. S. Melissas, G. C. Lynch, Y.-P. Liu, B. C. Garrett, R. Steckler, A. D. Isaacson, S. N. Rai, G. C. Hancock, J. G. Lauderdale, T. Joseph and D. G. Truhlar, *Computer Phys. Commun.* 71 (1992) 235.
- 73 R. Steckler, W.-P. Hu, Y.-P. Liu, G. C. Lynch, B. C. Garrett, A. D. Isaacson, V. S. Melissas, D.-h. Lu, T. N. Truong, S. N. Rai, G. C. Hancock, J. G. Lauderdale, T. Joseph and D. G. Truhlar, *Computer Phys. Commun.* 88 (1995) 341.
- 74 J. Zheng, J. L. Bao, R. Meana-Pañeda, S. Zhang, B. J. Lynch, J. C. Corchado, Y.-Y. Chuang, P. L. Fast, W.-P. Hu, Y.-P. Liu, G. C. Lynch, K. A. Nguyen, C. F. Jackels, A. Fernandez Ramos, B. A. Ellingson, V. S. Melissas, J. Villà, I. Rossi, E. L. Coitiño, J. Pu, T. V. Albu, A. Ratkiewicz, R. Steckler, B. C. Garrett, A. D. Isaacson and D. G. Truhlar, *Polyrate-version 2016-2A*, University of Minnesota, Minneapolis (2016).
- 75 D. G. Truhlar and A. Kuppermann, *Chem. Phys. Lett.* 9 (1971) 269.
- 76 B. C. Garrett, D. G. Truhlar, R. S. Grev and A. W. Magnuson, *J. Phys. Chem.* 84 (1980) 1730.
- 77 D. G. Truhlar and A. Kuppermann, *J. Am. Chem. Soc.* 93 (1971) 1840.
- 78 A. D. Isaacson and D. G. Truhlar, *J. Chem. Phys.* 76 (1982) 1380.
- 79 Y. Hida, X. S. Li and D. H. Bailey, *Library for double-double and quad-double arithmetic*, NERSC Division Lawrence Berkeley National Laboratory (2007).
- 80 M. Nakata, *The MPACK (MBLAS/MLAPACK); a multiple precision arithmetic version of BLAS and LAPACK, Version 0.6.7*, (2010). <http://mplapack.sourceforge.net>
- 81 J. A. Miller and S. J. Klippenstein, *Phys. Chem. Chem. Phys.* 15 (2013) 4744.
- 82 S. van der Walt, S. C. Colbert and G. Varoquaux, *Computing in Science & Engineering* 13 (2011) 22.
- 83 S. K. Lam, A. Pitrou and S. Seibert, *Proc. 2nd Workshop LLVM Compiler Infrastructure in HPC*, Austin, TX (2015) 6.
- 84 L. Dalcin, R. Paz, M. Storti and J. D'Elia, *J. Parallel Distributed Computing* 68 (2008). 655.

-
- 85 R. M. Zhang, D. G. Truhlar and X. Xu, *Research* (2019) 5373785.
- 86 X. Xu, E. Papajak, J. Zheng and D. G. Truhlar, *Phys. Chem. Chem. Phys.* 14 (2012) 4204.
- 87 L. Xing, J. L. Bao, Z. Wang, F. Zhang and D. G. Truhlar, *J. Am. Chem. Soc.* 139 (2017) 15821.
- 88 L. Xing, J. L. Bao, X. Wang, F. Zhang and D. G. Truhlar, *Combustion Flame* 197 (2018) 88.
- 89 L. Xing, J. L. Bao, Z. Wang, X. Wang and D. G. Truhlar, *J. Am. Chem. Soc.* 140 (2018) 17556.
- 90 T. C. Allison and D. G. Truhlar, in *Modern Methods for Multidimensional Dynamics Computations in Chemistry*, edited by D. L. Thompson (World Scientific, Singapore, 1998), pp. 618-712.
- 91 R.M. Zhang, X. Xu and D. G. Truhlar, *J. Am. Chem. Soc.* 142, 37 (2020) 16064.
- 92 D. G. Truhlar, A. D. Isaacson and B. C. Garrett, in *Theory of Chemical Reaction Dynamics*, edited by M. Baer (CRC Press, Boca Raton, FL, 1985), Vol. 4, pp. 65-137.